https://doi.org/10.5194/bg-2019-488
Preprint. Discussion started: 31 January 2020

Biogeosciences Discussions
Open Access
EGU

Factors controlling the competition between *Phaeocystis* and diatoms in the Southern Ocean

Cara Nissen[1] and Meike Vogt[1]

[1]Institute for Biogeochemistry and Pollutant Dynamics, ETH Zürich, Universitätstrasse 16, 8092 Zürich, Switzerland

Correspondence: C. Nissen (cara.nissen@usys.ethz.ch)

Abstract. The high-latitude Southern Ocean phytoplankton community is shaped by the competition between *Phaeocystis* and silicifying diatoms, with the relative abundance of these two groups controlling primary and export production, the production of dimethylsulfide, the ratio of silicic acid and nitrate available in the water column, and the structure of the food web. Here, we investigate this competition using a regional physical-biogeochemical-ecological model (ROMS-BEC) configured at eddy-permitting resolution for the Southern Ocean south of 35° S. We extended ROMS-BEC by an explicit parameterization of *Phaeocystis* colonies, so that the model, together with the previous addition of an explicit coccolithophore type, now includes all biogeochemically relevant Southern Ocean phytoplankton types. We find that *Phaeocystis* contribute 46% and 40% to annual NPP and POC export south of 60° S, respectively, making them an important contributor to high-latitude carbon cycling. In our simulation, the relative importance of *Phaeocystis* and diatoms is mainly controlled by the temporal variability in temperature and iron availability. The higher light sensitivity of *Phaeocystis* at low irradiances promotes the succession from *Phaeocystis* to diatoms in more coastal areas, such as the Ross Sea. Still, differences in the biomass loss rates, such as aggregation or grazing by zooplankton, need to be considered to explain the simulated seasonal biomass evolution.

1 Introduction

Unused nutrients from the Southern Ocean (SO) fuel global primary and export production (e.g. Sarmiento et al., 2004; Palter et al., 2010), and the amount and stoichiometry of these laterally exported nutrients is determined by multiple types of phytoplankton with different nutrient requirements. As on-going climate change alters the relative contribution of different phytoplankton groups to total net primary production (NPP; IPCC, 2014; Constable et al., 2014; Deppeler and Davidson, 2017), this will hence have ramifications for global biogeochemical cycles and food web structure (Smetacek et al., 2004). Today, the SO phytoplankton community is largely dominated by silicifying diatoms (e.g. Swan et al., 2016), but the contributions of calcifying coccolithophores and dimethylsulfide (DMS) producing *Phaeocystis* are substantial in the subantarctic (Balch et al., 2016; Nissen et al., 2018) and in the high latitudes, respectively (Smith and Gordon, 1997; Arrigo et al., 1999; DiTullio et al., 2000; Poulton et al., 2007), with a likely increase in the relative importance of the latter two types in a warming world (Bopp et al., 2005; Winter et al., 2013; Rivero-Calle et al., 2015). On a global scale, *Phaeocystis* has been suggested to be a major player in the marine cycling of DMS (e.g. Keller et al., 1989; Liss et al., 1994) and to contribute 6-65% to total phytoplankton carbon biomass (Buitenhuis et al., 2013b). Yet, the contribution of *Phaeocystis* to the export of particulate

https://doi.org/10.5194/bg-2019-488
Preprint. Discussion started: 31 January 2020


Biogeosciences Discussions Open Access EGU

organic carbon (POC) is still subject to debate. While some have found blooms of *Phaeocystis* to be important vectors of carbon transfer to depth through the formation of aggregates (Asper and Smith, 1999; DiTullio et al., 2000), others suggest their biomass losses to be efficiently degraded in the upper water column through bacterial and zooplankton activity, making *Phaeocystis* a minor contributor to POC export (Gowing et al., 2001; Accornero et al., 2003; Reigstad and Wassmann, 2007).

Possibly, the complex life cycle of *Phaeocystis* contributes to their apparent spatio-temporally varying relative importance for total biomass and POC export: Having a polymorphic life cycle, *Phaeocystis* alternates between solitary cells of a few μm in diameter and gelatinous colonies of several mm to cm in diameter (e.g. Rousseau et al., 1994; Peperzak, 2000; Chen et al., 2002), directly impacting community biomass partitioning and the fate of *Phaeocystis* biomass losses (Schoemann et al., 2005; Tang et al., 2008). While the factors controlling colony formation and disruption are still not fully clear (see review by Schoemann et al., 2005), the colonial form of *Phaeocystis* typically dominates over solitary cells in the SO growing season (Smith et al., 2003) and regionally and temporarily over diatoms in terms of carbon biomass (e.g. Smith and Gordon, 1997; Leblanc et al., 2012; Vogt et al., 2012).

To better quantify the effect of *Phaeocystis* on downward fluxes of carbon and nutrient distributions, factors controlling their biomass distributions need to be understood. In general, the relative importance of different phytoplankton types for total phytoplankton biomass is controlled by a combination of bottom-up, i.e. physical and biogeochemical variables impacting phytoplankton growth, and top-down factors, i.e. processes impacting phytoplankton loss such as grazing by zooplankton, aggregation of cells and subsequent sinking, or viral lysis (Le Quéré et al., 2016). Taking a bottom-up perspective, different phytoplankton types are often grouped in environmental niche space according to their preferred light and nutrient levels (Margalef, 1978; Reynolds, 2006). In the scheme by Reynolds (2006), R-strategists (low-light-high-nutrient) and S-strategists (high-light-low-nutrient) are found at opposite locations in the niche space. In this context, colonial and solitary cells of *Phaeocystis* can be grouped as R- and S-strategists, respectively, as *Phaeocystis* colonies are known to have a significantly lower affinity for nutrients, such as iron, than solitary cells (Veldhuis et al., 1991). Accordingly, colonial *Phaeocystis* are more similar to large diatoms, growing fast under nutrient/iron-replete conditions at relatively low light levels (see review by Schoemann et al., 2005). Consequently, the observed spatio-temporal differences in the relative importance of *Phaeocystis* and diatoms are thought to be largely controlled by differences in light and iron levels in the SO (Arrigo et al., 1998, 1999; Goffart et al., 2000; Sedwick et al., 2000; Garcia et al., 2009). A number of studies suggest *Phaeocystis* colonies to grow better than diatoms under low light levels (Garcia et al., 2009; Tang et al., 2009; Mills et al., 2010; Feng et al., 2010), implying a seasonal succession from *Phaeocystis* to diatoms throughout the growing season as light levels increase (Green and Sambrotto, 2006; Peloquin and Smith, 2007; Alvain et al., 2008). At the same time, in the Ross Sea, the large interannual variability in the relative importance of *Phaeocystis* and diatoms has been suggested to be due to the large variability in iron availability in summer (for the years 2001-2010, between 39-87% of the annual net community production is attributed to *Phaeocystis*, Smith et al., 2011, 2014). Therefore, iron availability may be more important in controlling the magnitude of the summer diatom bloom than the spring *Phaeocystis* bloom (Peloquin and Smith, 2007; Smith et al., 2011).

Yet, other studies suggest that top-down factors might be important in controlling the relative importance of *Phaeocystis* and diatoms. For instance, van Hilst and Smith (2002) suggest grazing by zooplankton to be an important factor explaining

https://doi.org/10.5194/bg-2019-488
Preprint. Discussion started: 31 January 2020

the observed distributions of these two phytoplankton types in the SO. In fact, grazing pressure has been shown to be lower on *Phaeocystis* colonies than on diatoms (Granéli et al., 1993; Smith et al., 2003; Tang et al., 2008), with cascading effects for food web structure (Smetacek et al., 2004). Furthermore, evidence also suggests a role for other biomass loss processes such as aggregation and subsequent sinking in controlling the relative abundance of *Phaeocystis* and diatoms (Asper and Smith, 1999). Altogether, this implies a complex interplay between bottom-up and top-down factors in controlling SO phytoplankton biomass levels in general and the relative importance of diatoms and *Phaeocystis* in particular, which is difficult to comprehensively assess through in situ studies.

Ecosystem models can be a useful tool to disentangle the controlling factors of SO phytoplankton biogeography over the course of the growing season and to quantify its biogeochemical implications (see e.g. Hashioka et al., 2013; Nissen et al., 2018). To date, some global (Wang and Moore, 2011; Le Quéré et al., 2016) or regional SO (Tagliabue and Arrigo, 2005; Pasquer et al., 2005; Kaufman et al., 2017) models exist that include an explicit representation of *Phaeocystis*, but these differ substantially in how they parameterize the life cycle of *Phaeocystis* (compare e.g. models including life cycle transitions such as Pasquer et al. (2005) and Kaufman et al. (2017) to Wang and Moore (2011) and Le Quéré et al. (2016), which only include the colonial stage of *Phaeocystis*). Using a 1D model setup for the Ross Sea, Kaufman et al. (2017) found light availability early in the growing season to critically impact the relative importance of diatoms and *Phaeocystis*. Similarly, in their study, Wang and Moore (2011) identify model parameters surrounding the light and iron sensitivity of growth by diatoms and *Phaeocystis* colonies to have the biggest impact on the relative importance of the two across the SO, with grazing by zooplankton playing only a minor role. While the models agree with the observations on the general importance of light and iron levels in controlling the relative importance of *Phaeocystis* and diatoms in the SO, a detailed quantitative analysis of the factors controlling the competition of these two phytoplankton types over the course of the growing season is missing. In the past, some of the above-mentioned models have been used to relate the simulated spatio-temporal variability in the high-latitude phytoplankton community structure to the simulated variability in air-sea CO_2 fluxes (at KERFIX and for the Ross Sea, see Pasquer et al., 2005; Tagliabue and Arrigo, 2005) or to quantify the contribution of *Phaeocystis* to the SO integrated annual NPP or POC export (23% and 30% south of 60° S, respectively, see Wang and Moore, 2011). Yet, none of these models has assessed the impacts of the seasonally varying phytoplankton community structure on basin-wide biogeochemical fluxes, such as POC export, and their implications for nutrient distributions.

In this study, we investigate the competition between *Phaeocystis* and diatoms using a regional coupled physical-biogeochemical-ecological model configured at eddy-permitting resolution for the SO (ROMS-BEC, Nissen et al., 2018). In our previous work (Nissen et al., 2018), we had already extended the original BEC model (Moore et al., 2013) with an explicit parametrization of coccolithophores. Now, we are adding *Phaeocystis* colonies as an additional phytoplankton functional type, so that the model includes all biogeochemically relevant phytoplankton types of the SO. We assess the relative importance of bottom-up and top-down factors in controlling the relative importance of *Phaeocystis* colonies and diatoms over a complete annual cycle in the high-latitude SO and the imprint of the relative importance of *Phaeocystis* on SO nutrient distributions. Furthermore, we quantify the impact of the simulated spatio-temporal variability in phytoplankton community structure on upper ocean carbon cycling and POC export.

https://doi.org/10.5194/bg-2019-488
Preprint. Discussion started: 31 January 2020

2 Methods

2.1 ROMS-BEC with explicit *Phaeocystis* colonies

We use a quarter-degree SO setup of the Regional Ocean Modeling System ROMS (latitudinal range from 24° S-78° S, 64 topography-following vertical levels, time step to solve the primitive equations is 1600 s; Shchepetkin and McWilliams, 2005; Haumann, 2016), coupled to the biogeochemical model BEC (Moore et al., 2013), which was recently extended to include an explicit represenation of coccolithophores and thoroughly validated in the SO setup (Nissen et al., 2018). BEC resolves the biogeochemical cycling of all macronutrients (C, N, P, Si), as well as the cycling of iron (Fe), the major micronutrient in the SO. The model includes four phytoplankton functional types (PFT) – diatoms, coccolithophores, small phytoplankton/SP, and N_2-fixing diazotrophs – and one zooplankton functional type (Moore et al., 2013; Nissen et al., 2018). Here, we extend the version of Nissen et al. (2018) to include an explicit parameterization of colonial *Phaeocystis antarctica*, which is the only species of *Phaeocystis* occurring in the SO (Schoemann et al., 2005). For the remainder of this manuscript, we will refer to the new PFT as "*Phaeocystis*". Generally, model parameters for *Phaeocystis* are chosen to represent the colonial form of *Phaeocystis* whenever information is available in the literature (see e.g. review by Schoemann et al., 2005). By only simulating the colonial form of *Phaeocystis*, we assume enough solitary cells of *Phaeocystis* to be available for colony formation at any time as part of the SP PFT. As for the other phytoplankton PFTs, growth by *Phaeocystis* is limited by surrounding temperature, nutrient, and light conditions as outlined in the following (for a complete description of the model equations describing phytoplankton growth, see Nissen et al., 2018).

As the new PFT in ROMS-BEC represents a single species of *Phaeocystis*, we use an optimum function to describe its temperature-limited growth rate $\mu^{\mathrm{PA}}(T)$ (d^{-1}, Schoemann et al., 2005):

$$\mu^{\mathrm{PA}}(T) = \mu^{\mathrm{PA}}_{\mathrm{max}} \cdot e^{-\left(\frac{T-T_{\mathrm{opt}}}{\tau}\right)^2} \quad (1)$$

In the above equation, the maximum growth rate ($\mu^{\mathrm{PA}}_{\mathrm{max}}$) is 1.56 d^{-1} at an optimum temperature (T_{opt}) of 3.6° C and the temperature interval (τ) is 17.51° C and 1.17° C at temperatures below and above 3.6° C, respectively. With these parameters, the simulated growth rate of *Phaeocystis* in ROMS-BEC is zero at temperatures above ∼8° C (in agreement with laboratory experiments with *Phaeocystis Antarctica*, see Buma et al., 1991) and higher than that of diatoms for temperatures between ∼0-4° C (Fig. A1a). We acknowledge that the range of temperatures for which the growth of *Phaeocystis* exceeds that of diatoms is possibly too small, as the temperature-limited growth rate by diatoms in ROMS-BEC is too high at low temperatures compared to available laboratory data (see Fig. A1a). Yet, we note that temperature-limited growth by diatoms in the model is tuned to fit the data at the global range of temperatures, in particular for the competition with coccolithophores at subantarctic latitudes (Nissen et al., 2018).

Half-saturation constants for macronutrient limitation are scarce for *P. antarctica* (Schoemann et al., 2005), and macronutrient limitation of *Phaeocystis* is therefore chosen to be identical to that of diatoms in ROMS-BEC (Table 1). As the availability of the micronutrient Fe generally limits phytoplankton growth in the high-latitude SO (Martin et al., 1990a, b) and accordingly in ROMS-BEC (Fig. S1), this choice is not expected to significantly impact the simulated competition between diatoms

https://doi.org/10.5194/bg-2019-488
Preprint. Discussion started: 31 January 2020

Biogeosciences Discussions Open Access EGU

Table 1. BEC parameters controlling phytoplankton growth and loss for the five phytoplankton PFTs diatoms (D), *Phaeocystis* (PA), coccolithophores (C), small phytoplankton (SP), and diazotrophs (N). Z=zooplankton, P=phytoplankton, PI=photosynthesis-irradiance. If not given in section 2.1, the model equations describing phytoplankton growth and loss rates are given in Nissen et al. (2018).

Parameter	Unit	Description	D	PA	C	SP	N†
$\mu_{\max}$	d^{-1}	max. growth rate at 30° C	4.6	‡	3.8	3.6	0.9
Q_{10}		temperature sensitivity	1.55	‡	1.45	1.5	1.5
k_{NO3}	mmol m^{-3}	half-saturation constant for NO_3	0.5	0.5	0.3	0.1	1.0
k_{NH4}	mmol m^{-3}	half-saturation constant for NH_4	0.05	0.05	0.03	0.01	0.15
k_{PO4}	mmol m^{-3}	half-saturation constant for PO_4	0.05	0.05	0.03	0.01	0.02
k_{DOP}	mmol m^{-3}	half-saturation constant for DOP	0.9	0.9	0.3	0.26	0.09
k_{Fe}	μmol m^{-3}	half-saturation constant for Fe	0.15	0.2	0.125	0.1	0.5
k_{SiO3}	mmol m^{-3}	half-saturation constant for SiO_3	1.0	-	-	-	-
α_{PI}	$\frac{\text{mmol C m}^2}{\text{mg Chl W s}}$	initial slope of PI-curve	0.44	0.63	0.4	0.44	0.38
$\gamma_{g,max}$	d^{-1}	max. growth rate of Z grazing on P	3.8	3.6	4.4	4.4	3.0
z_{grz}	mmol m^{-3}	half-saturation constant for ingestion	1.0	1.0	1.05	1.05	1.2
$\gamma_{m,0}$	d^{-1}	linear non-grazing mortality	0.12	0.18	0.12	0.12	0.15
$\gamma_{a,0}$	d^{-1}	quadratic mortality in aggregation	0.001	0.005	0.001	0.001	-
r_g	-	fraction of grazing routed to POC	0.3	0.42	0.2	0.05	0.05

† Compared to Nissen et al. (2018), the k_{Fe} of diazotrophs in ROMS-BEC is higher than for all other PFTs, consistent with literature reporting high Fe requirements of *Trichodesmium* (Berman-Frank et al., 2001). Furthermore, the maximum grazing rate on diazotrophs is lowest in the model (Capone, 1997). Still, diazotrophs continue to be a minor player in the SO phytoplankton community, contributing $<1\%$ to domain-integrated NPP in ROMS-BEC.

‡ The temperature-limited growth rate of *Phaeocystis* is calculated based on an optimum function according to Eq. 1 (see also Fig. A1a).

and *Phaeocystis* in this area. In contrast, differences in the half-saturation constants with respect to dissolved Fe concentrations (k_{Fe}) of *Phaeocystis* and diatoms possibly critically impact the competitive success of *Phaeocystis* relative to diatoms throughout the year (see e.g. Sedwick et al., 2000, 2007). Here, due to their larger size, we assume a higher k_{Fe} for *Phaeocystis* (0.2 μmol m^{-3}) than for diatoms (0.15 μmol m^{-3}, Table 1). We note however, that the k_{Fe} of *Phaeocystis* has been reported to vary over one order magnitude depending on the ambient light level (0.045-0.45 μmol m^{-3}, see Fig. A1b and Garcia et al., 2009), with lowest values at optimum light levels of around 80 W m^{-2}. Due to the limited number (3) of reported light levels in Garcia et al. (2009) and the associated uncertainty when fitting the data, we refrain from using this k_{Fe}-light-dependency in the *Baseline* simulation, but explore the sensitivity of the simulated seasonality of *Phaeocystis* and diatom biomass to a polynomial fit describing the k_{Fe} of *Phaeocystis* as a function of the light intensity (see Fig. A1b and section 2.2). As a result of the tuning exercise aiming to maximize the fit of *all* simulated PFT biomass fields to available observations, the k_{Fe} of the other PFTs in ROMS-BEC are increased by 25% in this study as compared to in Nissen et al. (2018, see Table 1). For diatoms, this change

https://doi.org/10.5194/bg-2019-488
Preprint. Discussion started: 31 January 2020

leads to a better agreement of the k_{Fe} used in ROMS-BEC with values suggested for large SO diatoms by Timmermans et al. (2004), but we acknowledge that the chosen value here is still at the lower end of their suggested range (0.19-1.14 μmol m^{-3}). We note that we currently do not include any luxury uptake of Fe by *Phaeocystis* into their gelatinous matrix (Schoemann et al., 2001). Serving as a storage of additional Fe accessible to the *Phaeocystis* colony when Fe in the seawater gets low, this luxury uptake is thought to relieve it from Fe limitation when Fe concentrations become growth limiting (see discussion in Schoemann et al., 2005). We therefore probably overestimate the Fe limitation of *Phaeocystis* growth in ROMS-BEC.

P. antarctica blooms are typically found where and when waters are comparatively turbulent and the mixed layer is comparatively deep (in comparison to blooms dominated by diatoms, see e.g. Arrigo et al., 1999; Alvain et al., 2008), suggesting that *Phaeocystis* is better in coping with low light levels than diatoms (e.g. Arrigo et al., 1999). In agreement with laboratory experiments (Tang et al., 2009; Mills et al., 2010; Feng et al., 2010), we therefore choose a higher α_{PI}, i.e. a higher sensitivity of growth to increases of photosynthetically active radiation (PAR) at low PAR levels, for *Phaeocystis* than for diatoms in ROMS-BEC (see Table 1). Our value (0.63 mmol C m^2 (mg Chl W s)$^{-1}$) corresponds to the average value compiled from available laboratory experiments (Schoemann et al., 2005).

In addition to environmental conditions directly impacting phytoplankton growth rates, loss processes such as grazing, non-grazing mortality, and aggregation impact the simulated biomass levels at any point and time. Grazing on *Phaeocystis* varies across zooplankton size classes, as a consequence of *Phaeocystis* life forms spanning several orders of magnitude in size (few μm to cm, Schoemann et al., 2005). Furthermore, *Phaeocystis* colonies are surrounded by a skin (Hamm et al., 1999), potentially serving as protection from zooplankton grazing. While small copepods have been shown to graze less on *Phaeocystis* once they form colonies, other larger zooplankton appear to continue grazing on *Phaeocystis* colonies at unchanged rates (Granéli et al., 1993; Schoemann et al., 2005; Nejstgaard et al., 2007). Based on a size-mismatch assumption of the single grazer in ROMS-BEC and *Phaeocystis* colonies, we assume a lower maximum grazing rate on *Phaeocystis* than on diatoms (3.6 d^{-1} and 3.8 d^{-1}, respectively, see $\gamma_{g,max}$ in Table 1). Upon grazing, we assume the fraction of the grazed phytoplankton biomass that is transformed to sinking POC via zooplankton fecal pellet production to be higher for larger and ballasted cells. Consequently, the fraction of grazing routed to POC increases from grazing on SP or diazotrophs to coccolithophores, *Phaeocystis*, and diatoms (r_g in Table 1). Consistent with Nissen et al. (2018), we keep a Holling Type II ingestion functional response here and compute grazing on each prey separately. We refer to Nissen et al. (2018) for a discussion of the relative merits and pitfalls for using Holling Type II versus III.

Non-grazing mortality (such as viral lysis) has been shown to increase under environmental stress for *Phaeocystis* colonies, causing colony disruption and ultimately cell death (van Boekel et al., 1992; Schoemann et al., 2005). To account for processes causing colony disintegration and for grazing by higher trophic levels not explicitly included in ROMS-BEC, *Phaeocystis* in ROMS-BEC experience a higher mortality rate than diatoms (0.18 d^{-1} and 0.12 d^{-1}, respectively, see $\gamma_{m,0}$ in Table 1). Thereby, the chosen non-grazing mortality rate of *Phaeocystis* assumed in the model is still lower than the estimated rate of viral lysis for *Phaeocystis* in the North Sea by van Boekel et al. (1992, 0.25 d^{-1}), but we note that data on non-grazing mortality of *P. antarctica* are currently lacking (Schoemann et al., 2005). Furthermore, based on the assumption that for a given biomass

https://doi.org/10.5194/bg-2019-488
Preprint. Discussion started: 31 January 2020

Table 2. Overview of sensitivity experiments aiming to assess the sensitivity of the simulated *Phaeocystis*-diatom competition to chosen parameter values and parameterizations of *Phaeocystis*. See Table 1 and section 2.1 for parameter values and parameterizations of *Phaeocystis* in the reference simulation. PA=*Phaeocystis*, D=diatoms.

	Run Name	**Description**
1	TEMPERATURE	Use $\mu^{\mathrm{D}}_{\mathrm{max}}$, $\mathrm{Q}^{\mathrm{D}}_{10}$, and $\mu^{\mathrm{PA}}_{\mathrm{T}} = \mu^{\mathrm{D}}_{\mathrm{max}} \cdot \mathrm{Q}^{\mathrm{D}}_{10}{}^{\frac{\mathrm{T}-\mathrm{T}_{\mathrm{ref}}}{10^{\circ}\mathrm{C}}}$ to compute the temperature-limited growth rate of *Phaeocystis* instead of Eq. 1
2	$\mathrm{ALPHA}_{\mathrm{PI}}$	Set $\alpha^{\mathrm{PA}}_{\mathrm{PI}}$ to $\alpha^{\mathrm{D}}_{\mathrm{PI}}$
3	IRON	Set $\mathrm{k}^{\mathrm{PA}}_{\mathrm{Fe}}$ to $\mathrm{k}^{\mathrm{D}}_{\mathrm{Fe}}$
4	GRAZING	Set $\gamma^{\mathrm{PA}}_{\mathrm{g,max}}$ to $\gamma^{\mathrm{D}}_{\mathrm{max}}$
5	AGGREGATION	Set $\gamma^{\mathrm{PA}}_{\mathrm{a},0}$ to $\gamma^{\mathrm{D}}_{\mathrm{a},0}$
6	MORTALITY	Set $\gamma^{\mathrm{PA}}_{\mathrm{m},0}$ to $\gamma^{\mathrm{D}}_{\mathrm{m},0}$
7	VARYING_kFE	Use $\mathrm{k}^{\mathrm{PA}}_{\mathrm{Fe}}(\mathrm{I}) = 2.776 \cdot 10^{-5} \cdot (\mathrm{I} + 20)^2$ - 0.00683 · (I + 20) + 0.46 (with the irradiance I in W m^{-2}) instead of a constant $\mathrm{k}^{\mathrm{PA}}_{\mathrm{Fe}}$

concentration, larger cells are more likely than smaller cells to form aggregates and subsequently sink as POC, we use a higher quadratic mortality rate for *Phaeocystis* (0.005 d^{-1}) than for diatoms (0.001 d^{-1}) in the model (see $\gamma_{\mathrm{a},0}$ in Table 1).

In summary, the spatio-temporal variability of the relative importance of *Phaeocystis* and diatoms in ROMS-BEC is controlled by the interplay of the environmental conditions and loss processes, which differentially impact the growth and loss rates of these two PFTs and consequently their competitive fitness in the model. In the following, we will describe the model setup and the simulations that were performed to assess the competition between *Phaeocystis* and diatoms throughout the year in the high-latitude SO. The simulations include a set of sensitivity experiments, with the aim to assess the impact of choices of single parameters or parameterizations on the simulated *Phaeocystis* biogeography.

2.2 Model setup and simulations

With few exceptions, we use the same ROMS-BEC model setup as described in detail in Nissen et al. (2018): At the open northern boundary, we use monthly climatological fields for all tracers (Carton and Giese, 2008; Locarnini et al., 2013; Zweng et al., 2013; Garcia et al., 2014b, a; Lauvset et al., 2016; Yang et al., 2017), and the same data sources are used to initialize the model simulations. At the ocean surface, the model is forced with a 2003-normal year forcing for momentum, heat, and freshwater fluxes (Dee et al., 2011). Satellite-derived climatological total chlorophyll concentrations are used to initialize phytoplankton biomass and to constrain it at the open northern boundary in the model (NASA-OBPG, 2014b), and the fields are extrapolated to depth following Morel and Berthon (1989). Due to the addition of *Phaeocystis*, the partitioning of total chlorophyll onto the different phytoplankton PFTs is adjusted compared to Nissen et al. (2018): 90% is attributed to small phytoplankton, 4% to diatoms and coccolithophores, respectively, and 1% to diazotrophs and *Phaeocystis*, respectively. This

https://doi.org/10.5194/bg-2019-488
Preprint. Discussion started: 31 January 2020

partitioning is motivated by the phytoplankton community structure at the open northern boundary at 24° S, where small phytoplankton typically dominate and *P. Antarctica* are only a minor contributor to phytoplankton biomass (see e.g. Schoemann et al., 2005; Swan et al., 2016). *Phaeocystis* is initialized with a carbon-to-chlorophyll ratio of 60 mg C (mg chl)$^{-1}$ (same as small phytoplankton and coccolithophores), whereas diatoms are initialized with a ratio of 36 mg C (mg chl)$^{-1}$ (Sathyendranath et al., 2009).

We first run a 30 year long physics-only spin-up, followed by a 10 year long spin-up in the coupled ROMS-BEC setup. Our *Baseline* simulation for this study is then run for an additional 10 years, of which we analyze a daily climatology over the last 5 full seasonal cycles. i.e. from 1 July of year 5 until 30 June of year 10. Apart from having added *Phaeocystis* and adjusted the parameters of the other PFTs as described in section 2.1, the setup of the *Baseline* simulation in this study is thereby identical to the *Baseline* simulation in Nissen et al. (2018). We will evaluate the model's performance with respect to the simulated phytoplankton biogeography in section 3.1 and in the supplementary material.

Furthermore, we perform seven sensitivity experiments, in order to assess the sensitivity of the simulated *Phaeocystis* biogeography and the competition of *Phaeocystis* and diatoms to chosen parameters and parameterizations (Table 2). To do so, we set the parameters and parameterizations of *Phaeocystis* to those used for diatoms in ROMS-BEC (runs 1-6 in Table 2). Generally, the differences in parameters between *Phaeocystis* and diatoms affect either the simulated growth rates (runs TEMPERATURE, $\mathrm{ALPHA_{PI}}$, and IRON) or loss rates (runs GRAZING, AGGREGATION, and MORTALITY). By successively eradicating the differences between *Phaeocystis* and diatoms, these simulations allow us to directly quantify the impact of differences in parameters on the simulated relative importance of *Phaeocystis* for total phytoplankton biomass. To assess the impact of iron-light interactions on the competitive success of *Phaeocystis* at high SO latitudes, we ultimately run a simulation in which the half-saturation constant of iron ($\mathrm{k_{Fe}}$) of *Phaeocystis* is a function of the light intensity, following a polynomial fit of available laboratory data (VARYING_kFE, see Fig. A1b and Garcia et al., 2009). All sensitivity experiments use the same physical spin-up as the *Baseline* simulation and start from the end of year 10 of the *Baseline* simulation. Each simulation is then run for an additional 10 years, of which the average over the last 5 full seasonal cycles is analyzed in this study.

2.3 Analysis framework

2.3.1 Evaluating the simulated phytoplankton community structure

We compare the simulated spatio-temporal variability in phytoplankton biomass and community structure to available observations of phytoplankton carbon biomass concentrations from the MAREDAT initiative (O'Brien et al., 2013; Leblanc et al., 2012; Vogt et al., 2012), satellite-derived total chlorophyll concentrations (Fanton d'Andon et al., 2009; Maritorena et al., 2010), DMS measurements (Curran and Jones, 2000; Lana et al., 2011), the ecological niches suggested for SO phytoplankton taxa (Brun et al., 2015), and the CHEMTAX climatology based on high performance liquid chromatography (HPLC) pigment data (Swan et al., 2016). The latter provides seasonal estimates of the mixed layer average community composition, which we compare to the seasonally and top 50 m averaged model output of each phytoplankton's contribution to total chlorophyll biomass. The CHEMTAX analysis splits the phytoplankton community into diatoms, nitrogen fixers (such as *Trichodesmium*),

https://doi.org/10.5194/bg-2019-488
Preprint. Discussion started: 31 January 2020

pico-phytoplankton (such as *Synechococcus* and *Prochlorococcus*), dinoflagellates, cryptophytes, chlorophytes (all three combined into the single group "Others" here), and haptophytes (such as coccolithophores and *Phaeocystis*). As noted in Swan et al. (2016), the differentiation between coccolithophores and *Phaeocystis* in the CHEMTAX analysis is difficult and prone to error. Possibly, this is due to the large variability in pigment composition of *Phaeocystis* as a response to varying environmental conditions, especially regarding light and iron levels (Smith et al., 2010; Wright et al., 2010). Coccolithophores have been reported to only grow very slowly at low temperatures (below $\sim 8^{\circ}$ C, Buitenhuis et al., 2008), and in the SO, their abundance in the high latitudes south of the polar front is very low (Balch et al., 2016). Therefore, whenever the climatological temperature in the World Ocean Atlas 2013 (Locarnini et al., 2013) is below 2° C at the time and location of the respective HPLC observation, we re-assign data points identified as "Hapto-6" (hence e.g. *Emiliania huxleyi*) in the CHEMTAX analysis to "Hapto-8" (hence e.g. *Phaeocystis Antarctica*). Throughout the manuscript, this new category ("Hapto-8 re-assigned") is indicated separately in the respective figures, and leads to a better correspondence of the functional types included in the CHEMTAX-based climatology by Swan et al. (2016) and the PFTs in ROMS-BEC.

To assess the controlling factors of the simulated PFT distributions in our model, we analyze the simulated December-March (DJFM) top 50 m average biomass distribution of the different model PFTs south of 40° S in environmental niche space. To that aim, we bin the simulated carbon biomass concentrations of *Phaeocystis*, diatoms, and coccolithophores in ROMS-BEC as a function of the temperature [$^{\circ}$ C], nitrate concentration [mmol m^{-3}], iron concentration [μmol m^{-3}], and mixed layer photosynthetically active radiation (MLPAR; W m^{-2}). Subsequently, we compare the simulated ecological niche to that observed for example taxa from the SO of each model PFT (such as *Phaeocystis Antarctica*, *Fragilariopsis kerguelensis*, *Thalassiosira* sp., or *Emiliania huxleyi*, see Brun et al., 2015). While this analysis informs on possible links between the competitive fitness of a PFT and the environmental conditions it lives in, the assessment is hindered due to difficulties in comparing a model PFT to individual phytoplankton species, a sampling bias towards the summer months and the low latitudes, and the neglect of loss processes such as zooplankton grazing to explain biomass distributions. As a consequence, the ecological niche analysis does not allow for the assessment of any temporal variability in PFT biomass concentrations.

In order to assess the simulated seasonality and the seasonal succession of *Phaeocystis* and diatoms, we identify the bloom peak as the day of peak chlorophyll concentrations throughout the year. Besides the timing of the bloom peak, phytoplankton phenology is typically characterized by metrics such as the day of bloom initiation or the day of bloom end (see e.g. Soppa et al., 2016). In this regard, the timing of the bloom start is known to be sensitive to the chosen identification methodology (Thomalla et al., 2015). At high latitudes, the identification of the bloom start based on remotely sensed chlorophyll concentrations is additionally impaired by the large number of missing data in all seasons (even in the summer months, a large part of the SO is sampled by the satellite in less than 5 of the 21 available years, see Fig. S2), complicating any comparison of the high-latitude satellite-derived bloom start with output from models such as ROMS-BEC. To minimize the uncertainty due to the low data coverage in the region of interest for this study, and as the seasonal succession of *Phaeocystis* and diatoms in the high-latitude SO is mostly inferred from the timing of observed maximum abundances in the literature (e.g. Peloquin and Smith, 2007; Smith et al., 2011), we focus our discussion of the simulated bloom phenology on the timing of the bloom peak. To evaluate the model's performance, we compare the timing of the total chlorophyll bloom peak in the *Baseline* simulation of ROMS-BEC

https://doi.org/10.5194/bg-2019-488
Preprint. Discussion started: 31 January 2020

to the bloom timing derived from climatological daily chlorophyll data from Globcolor (climatology from 1998-2018 based on the daily 25 km chlorophyll product, see Fanton d'Andon et al., 2009; Maritorena et al., 2010).

The release of dimethylsulfoniopropionate (DMSP) via zooplankton grazing, cell lysis, and exudation and the subsequent transformation to DMS by bacterial activity are the major sources of DMS in seawater (e.g. Stefels et al., 2007). With *Phaeocystis* being the major DMSP producer in the SO (Keller et al., 1989; Liss et al., 1994), the timing of observed peak seawater DMS concentrations (Curran et al., 1998; Curran and Jones, 2000) will allow us to assess the simulated seasonality of *Phaeocystis* in the model. Though not explicitly including the biogeochemical cycling of sulphur, we can nevertheless use model output from ROMS-BEC to obtain an estimate of DMS production by *Phaeocystis* through a simple back-of-the-envelope calculation. To this aim, we use the model-based *Phaeocystis* biomass loss rates via zooplankton grazing and non-grazing mortality to get the DMSP release from this PFT (integrated annually over the top 10 m; we neglect exudation here), a molar DMSP:C ratio for *Phaeocystis* of 0.011 (Stefels et al., 2007), and a DMSP-to-DMS conversion efficiency between 0.2-0.7 (the DMS yield depends on the local sulphur demand of bacteria, Stefels et al., 2007; Wang et al., 2015). By comparing the resulting model-based estimates to previously published global estimates of marine DMS emissions (Lana et al., 2011), we obtain an estimate of the importance of SO *Phaeocystis* for global sulphur cycling.

2.3.2 Assessing phytoplankton competition throughout the year

In ROMS-BEC, phytoplankton biomass P^{i} (mmol C m^{-3}, $i \in \{PA, D, C, SP, N\}$) is the balance between growth (μ^{i}) and loss terms (grazing by zooplankton $\gamma^{\mathrm{i}}_{\mathrm{g}}$, non-grazing mortality $\gamma^{\mathrm{i}}_{\mathrm{m}}$, and aggregation $\gamma^{\mathrm{i}}_{\mathrm{a}}$, see appendix in Nissen et al. (2018) for a full description of the model equations). Here, in order to disentangle the factors controlling the relative importance of *Phaeocystis* and diatoms for total phytoplankton biomass throughout the year, we use the metrics first introduced by Hashioka et al. (2013) and then applied to assess the competition of diatoms and coccolithophores in ROMS-BEC in Nissen et al. (2018). Same as in Nissen et al. (2018), the relative growth ratio $\mu^{\mathrm{ij}}_{\mathrm{rel}}$ of phytoplankton i and j (e.g. diatoms and *Phaeocystis*) is defined as the ratios of their specific growth rates (μ^{i}, d^{-1}), which in turn depends on environmental dependencies regarding the temperature T, nutrients N, and irradiance I, following:

$$\begin{aligned}\mu^{\mathrm{DPA}}_{\mathrm{rel}} &= \log \frac{\mu^{\mathrm{D}}}{\mu^{\mathrm{PA}}} \\ &= \underbrace{\log \frac{\mathrm{f^D(T)} \cdot \mu^{\mathrm{D}}_{\mathrm{max}}}{\mu^{\mathrm{PA}}_{\mathrm{T}}}}_{\beta_T} + \underbrace{\log \frac{\mathrm{g^D(N)}}{\mathrm{g^{PA}(N)}}}_{\beta_{\mathrm{N}} \sim \beta_{\mathrm{Fe}}} + \underbrace{\log \frac{\mathrm{h^D(I)}}{\mathrm{h^{PA}(I)}}}_{\beta_{\mathrm{I}}}\end{aligned} \tag{2}$$

In the above equation, the specific growth rate μ^{i} of each phytoplankton i is calculated as a multiplicative function of a temperature-limited growth rate ($\mathrm{f^D(T)} \cdot \mu^{\mathrm{D}}_{\mathrm{max}}$ for diatoms and $\mu^{\mathrm{PA}}_{\mathrm{T}}$ for *Phaeocystis*, see Eq. 1), a nutrient limitation term ($\mathrm{g^i(N)}$, limitation of each nutrient is calculated using a Michaelis-Menten function, and the most-limiting one is then used here), and a light limitation term ($\mathrm{h^i(I)}$, Geider et al., 1998). For a detailed description of the underlying functions $f(T)$, $g(N)$, and $h(I)$, the reader is referred to the appendix in Nissen et al. (2018). At high-latitudes south of 60° S, the ratio of the nutrient limitation of growth β_{N} corresponds to that of the iron limitation β_{Fe} in our model (Fig. S1). Consequently, environmental

https://doi.org/10.5194/bg-2019-488
Preprint. Discussion started: 31 January 2020

conditions regarding temperature, iron, and light decide whether the relative growth ratio is positive or negative at a given location and point in time, i.e., which of the two phytoplankton types has a higher specific growth rate and hence a competitive advantage over the other regarding growth.

Similarly, the relative grazing ratio $\gamma^{\mathrm{ij}}_{\mathrm{g,rel}}$ of phytoplankton i and j (e.g. diatoms and *Phaeocystis*) is defined as the ratio of their specific grazing rates ($\gamma^{\mathrm{i}}_{\mathrm{g}}$, d^{-1}) following:

$$\gamma^{\mathrm{DPA}}_{\mathrm{g,rel}} = \log \frac{\frac{\gamma^{\mathrm{PA}}_{\mathrm{g}}}{P^{\mathrm{PA}}}}{\frac{\gamma^{\mathrm{D}}_{\mathrm{g}}}{P^{\mathrm{D}}}} \tag{3}$$

In ROMS-BEC, grazing on each phytoplankton i is calculated using a Holling Type II ingestion function (Nissen et al., 2018). As described in section 2.1, *Phaeocystis* and diatoms in ROMS-BEC do not only differ in parameters describing the zooplankton grazing pressure they experience, but in parameters describing their non-grazing mortality and aggregation losses as well. Therefore, in accordance with the relative grazing ratio defined above, we define the relative mortality ratio ($\gamma^{\mathrm{ij}}_{\mathrm{m,rel}}$) and the relative aggregation ratio ($\gamma^{\mathrm{ij}}_{\mathrm{a,rel}}$) of phytoplankton i and j (e.g. diatoms and *Phaeocystis*) as the ratio of their specific non-grazing mortality rates ($\gamma^{\mathrm{i}}_{\mathrm{m}}$, d^{-1}) and aggregation rates ($\gamma^{\mathrm{i}}_{\mathrm{a}}$, d^{-1}), respectively, following:

$$\gamma^{\mathrm{DPA}}_{\mathrm{m,rel}} = \log \frac{\frac{\gamma^{\mathrm{PA}}_{\mathrm{m}}}{P^{\mathrm{PA}}}}{\frac{\gamma^{\mathrm{D}}_{\mathrm{m}}}{P^{\mathrm{D}}}} \tag{4}$$

$$\gamma^{\mathrm{DPA}}_{\mathrm{a,rel}} = \log \frac{\frac{\gamma^{\mathrm{PA}}_{\mathrm{a}}}{P^{\mathrm{PA}}}}{\frac{\gamma^{\mathrm{D}}_{\mathrm{a}}}{P^{\mathrm{D}}}} \tag{5}$$

Since the total specific loss rate ($\gamma^{\mathrm{ij}}_{\mathrm{total}}$, d^{-1}) of phytoplankton i is the addition of its specific grazing, non-grazing mortality, and aggregation loss rates, the relative total loss ratio $\gamma^{\mathrm{ij}}_{\mathrm{total,rel}}$ of phytoplankton i and j (e.g. diatoms and *Phaeocystis*) is defined as

$$\gamma^{\mathrm{DPA}}_{\mathrm{total,rel}} = \log \frac{\frac{\gamma^{\mathrm{PA}}_{\mathrm{g}}}{P^{\mathrm{PA}}} + \frac{\gamma^{\mathrm{PA}}_{\mathrm{m}}}{P^{\mathrm{PA}}} + \frac{\gamma^{\mathrm{PA}}_{\mathrm{a}}}{P^{\mathrm{PA}}}}{\frac{\gamma^{\mathrm{D}}_{\mathrm{g}}}{P^{\mathrm{D}}} + \frac{\gamma^{\mathrm{D}}_{\mathrm{m}}}{P^{\mathrm{D}}} + \frac{\gamma^{\mathrm{D}}_{\mathrm{a}}}{P^{\mathrm{D}}}} \tag{6}$$

If $\gamma^{\mathrm{DPA}}_{\mathrm{total,rel}}$ is positive, the specific total loss rate of *Phaeocystis* is larger than that of diatoms (and accordingly for the individual loss ratios in Eq. 3-5), and loss processes promote the accumulation of diatom biomass relative to that of *Phaeocystis*. While the maximum grazing rate on *Phaeocystis* is lower than that of diatoms, their non-grazing mortality and aggregation losses are higher (see section 2.1 and Table 1). Ultimately, at any given location and point in time, the interaction between the phytoplankton biomass concentrations (impacting the respective loss rates) and environmental conditions (impacting the respective growth rate) will determine the relative contribution of each phytoplankton type i to total phytoplankton biomass. Here, we use these metrics to assess the controls on the simulated seasonal evolution of the relative importance of *Phaeocystis* and diatoms in the high-latitude SO.

https://doi.org/10.5194/bg-2019-488
Preprint. Discussion started: 31 January 2020

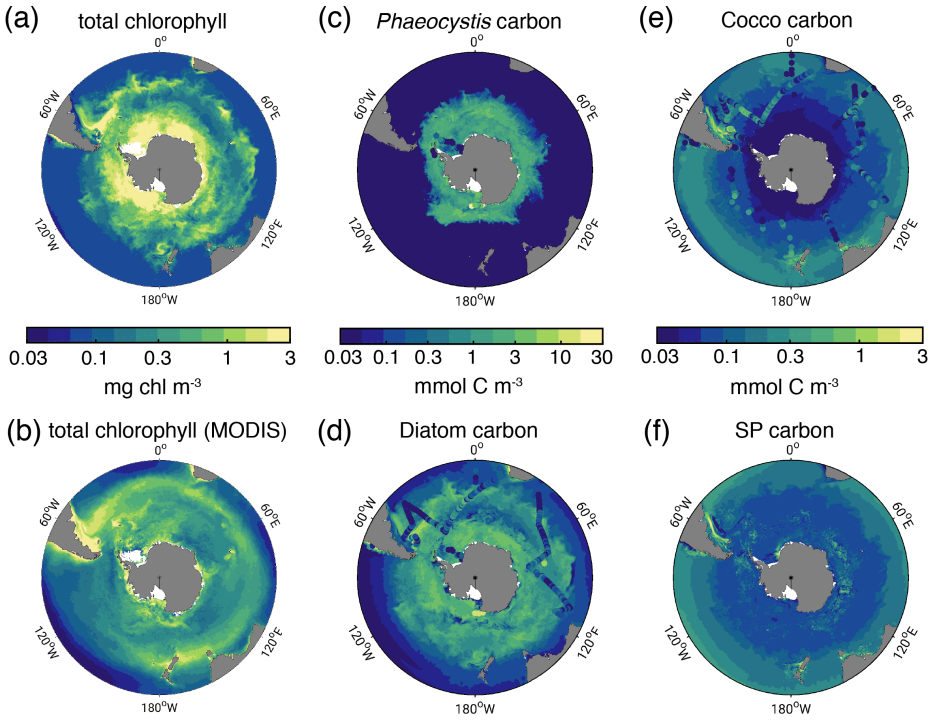

Figure 1. Biomass distributions for December-March (DJFM). Total surface chlorophyll [mg chl m^{-3}] in a) ROMS-BEC and b) MODIS-Aqua climatology (NASA-OBPG, 2014a), using the chlorophyll algorithm by Johnson et al. (2013). c)-f) Mean top 50 m c) *Phaeocystis*, d) diatom, e) coccolithophore, and f) small phytoplankton carbon biomass concentrations [mmol C m^{-3}] in ROMS-BEC. *Phaeocystis*, diatom, and coccolithophore biomass observations from the top 50 m are indicated by colored dots in c), d), and e), respectively (Balch et al., 2016; Saavedra-Pellitero et al., 2014; O'Brien et al., 2013; Vogt et al., 2012; Leblanc et al., 2012; Tyrrell and Charalampopoulou, 2009; Gravalosa et al., 2008; Cubillos et al., 2007). For more details on the biomass evaluation, see Nissen et al. (2018).

3 Results

3.1 Phytoplankton biogeography and community composition in the SO

In ROMS-BEC, total summer chlorophyll is highest close to the Antarctic continent (>10 mg chl m^{-3}) and decreases northwards to values <1 mg chl m^{-3} close to the open northern boundary (Fig. 1a). While this south-north gradient is in broad agreement with remotely sensed chlorophyll concentrations (Fig. 1b), our model generally overestimates high-latitude chlorophyll levels, which has already been noted for the 4-PFT setup of ROMS-BEC (Nissen et al., 2018). With *Phaeocystis* added, the model overestimates annual mean satellite derived surface chlorophyll biomass estimates by 18% (40.8 Gg chl in ROMS-BEC between 30-90° S compared to 34.5 Gg chl in the MODIS Aqua chlorophyll product, Table 3, NASA-OBPG, 2014a; Johnson et al., 2013) and satellite derived NPP by 38-42% (17.2 compared to 12.1-12.5 Pg C yr^{-1}, Table 3, Behrenfeld and Falkowski, 1997; O'Malley, last access: 16 May 2016; Buitenhuis et al., 2013a). This bias is largest south of 60° S, where NPP

https://doi.org/10.5194/bg-2019-488
Preprint. Discussion started: 31 January 2020

Table 3. Comparison of ROMS-BEC based phytoplankton biomass, production, and export estimates with available observations (given in parentheses). Data sources are given below the Table.

		ROMS-BEC (Data)	
		30-90° S	**60-90° S**
Surface chlorophyll biomass	total, annual mean [Gg chl]	40.8 (34.5[a])	17.1 (9.5[a])
Diatom carbon biomass	0-200m, annual mean [Pg C]	0.059 (global[b]: 0.10-0.94)	0.015
Phaeocystis carbon biomass	0-200m, annual mean [Pg C]	0.019 (global[b]: 0.11-0.71)	0.010
Coccolithophore carbon biomass	0-200m, annual mean [Pg C]	0.012 (global[b]: 0.001-0.03)	0.001
NPP	Pg C yr^{-1}	17.2 (12.1-12.5[c])	3.0 (0.68-1.7[c])
	Diatoms [%]	52.0	49.1
	Phaeocystis [%]	15.3	45.8
	Coccolithophores [%]	14.6	0.7
	SP [%]	17.2	4.5
POC export at 100m	Pg C yr^{-1}	3.1 (2.3-2.96[d])	0.62 (0.21-0.24[d])

[a] Monthly climatology from MODIS Aqua (2002-2016, NASA-OBPG, 2014a), SO algorithm (Johnson et al., 2013)
[b] The reported estimates from the MAREDAT data base in Buitenhuis et al. (2013) are global estimates of phytoplankton biomass.
[c] Monthly climatology from MODIS Aqua VGPM (2002-2016, Behrenfeld and Falkowski, 1997; O'Malley, last access: 16 May 2016), NPP climatology from Buitenhuis et al. (2013a, 2002-2016)
[d] Monthly output from a biogeochemical inverse model (Schlitzer, 2004) and a data-assimilated model (DeVries and Weber, 2017).

and surface chlorophyll are overestimated by a factor 1.8-4.4 and 1.8, respectively (Table 3), and the bias is likely due to a combination of underestimated high-latitude chlorophyll concentrations in satellite-derived products (Johnson et al., 2013) and the missing complexity in the zooplankton compartment in ROMS-BEC, as biases in the simulated physical fields (temperature, light) have been shown to only explain a minor fraction of the simulated high-latitude biomass overestimation (Nissen et al., 2018).

The simulated carbon biomass distributions of colonial *Phaeocystis*, diatoms, coccolithophores, and SP are distinctly different in the model (Fig. 1c-f, showing top 50 m averages). The simulated summer *Phaeocystis* biomass is highest south of 50° S (top 50 m mean), with highest concentrations of 10 mmol C m^{-3} at ∼74° S. In the model, average *Phaeocystis* biomass concentrations quickly decline to levels <0.1 mmol C m^{-3} north of 50° S (Fig. 1c), a direct result of the restriction of *Phaeocystis* growth to temperatures < ∼8° C in the model (Fig. A1a). This is in broad agreement with in situ observations, which suggest highest concentrations (>20 mmol C m^{-3}) south of ∼75° S, and concentrations <5 mmol C m^{-3} north of ∼65° S (Fig. 1c & Fig. S3a & b). As a response to the addition of *Phaeocystis* to ROMS-BEC, the simulated high-latitude diatom biomass concentrations decrease compared of the 4-PFT setup of the model (Nissen et al., 2018). In the 5-PFT setup, the model simulates highest diatom biomass south of 60° S with maximum concentrations of ∼7 mmol C m^{-3} at 72° S (top 50 m mean; ∼17 mmol C m^{-3} in 4-PFT setup) and rapidly declining concentrations north of 60° S (Fig. 1d). Nevertheless, the simulated summer diatom biomass levels are still overestimated compared to carbon biomass estimates (Fig. S3c, Leblanc et al., 2012)

https://doi.org/10.5194/bg-2019-488
Preprint. Discussion started: 31 January 2020

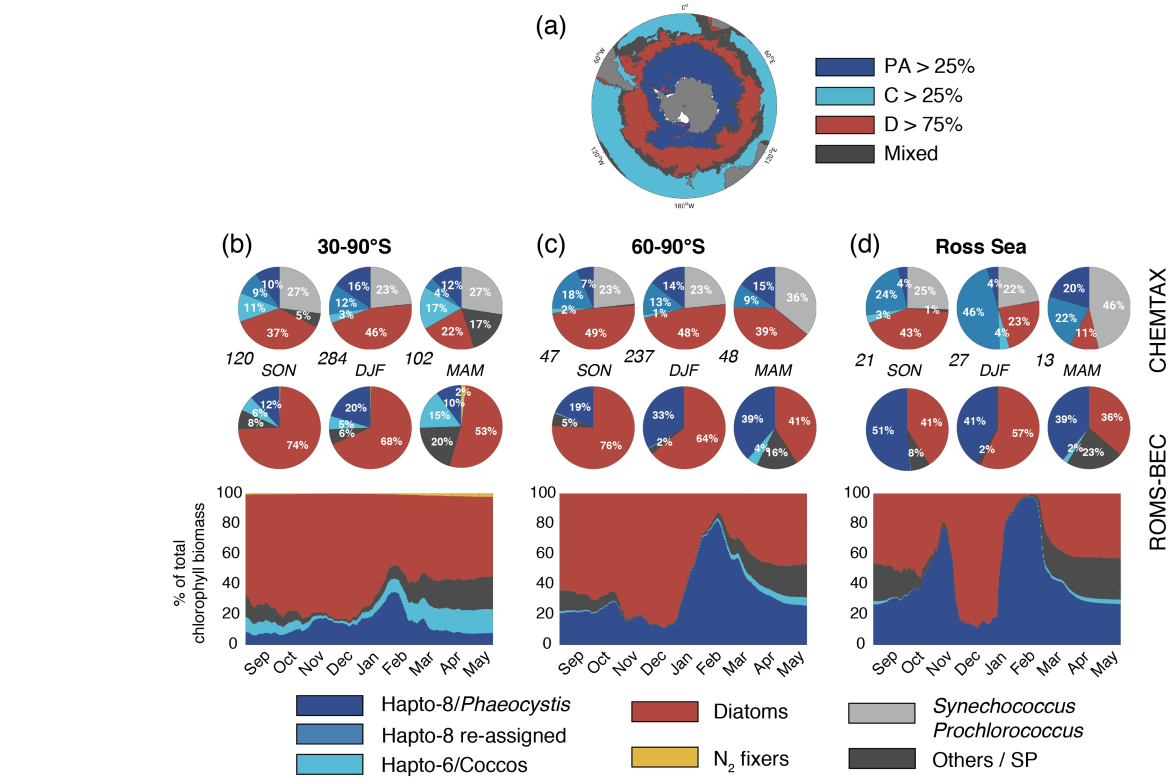

Figure 2. Spatio-temporal distribution of phytoplankton communities in the SO. a) Diatom-dominated phytoplankton community vs. mixed communities with substantial contributions of *Phaeocystis*, coccolithophores and small phytoplankton in ROMS-BEC. Communities in which neither *Phaeocystis* (PA, dark blue) or coccolithophores (C, light blue) contribute >25 % nor diatoms (D, red) contribute >75 % to total annual NPP are classified as mixed communities (grey). b)-d) Relative contribution of the five phytoplankton PFTs to total chlorophyll biomass [mg chl m^{-3}] for b) 30-90° S, c) 60-90° S, and d) the Ross Sea. The top pie charts denote the climatological mixed layer average community composition suggested by CHEMTAX analysis of HPLC pigments for spring, summer, and fall, respectively (the total number of available observations for a given region and season is given at the lower left side, Swan et al., 2016), and the lower pie charts denote the corresponding community structure in the top 50 m in ROMS-BEC. Note that the categories in the CHEMTAX analysis are not 100% equivalent to the model PFTs, and here, "Hapto-8 reassigned" corresponds to the contribution of Hapto-6 where the temperature is <2° C (see also section 2.3.1). The panels at the bottom denote the daily contribution of each PFT in ROMS-BEC to total surface chlorophyll biomass.

and satellite derived diatom chlorophyll estimates (Soppa et al., 2014, comparison not shown). In contrast to both *Phaeocystis* and diatoms, the simulated biomass levels of coccolithophores are highest in the subantarctic (highest concentrations of 3 mmol C m^{-3} on the Patagonian Shelf, Fig. 1e & S3d), and their simulated SO biogeography remains largely unchanged compared to the 4-PFT setup (Nissen et al., 2018).

https://doi.org/10.5194/bg-2019-488
Preprint. Discussion started: 31 January 2020

Taken together, the model simulates a phytoplankton community with substantial contributions of coccolithophores and *Phaeocystis* in the subantarctic and high-latitude SO, respectively (Fig. 2a). CHEMTAX data generally support this latitudinal trend (CHEMTAX is based on high performance liquid chromatography pigment data, see Fig. 2b-d and section 2.3.1, Swan et al., 2016). Averaged over 30-90° S (60-90° S), the simulated relative contributions of *Phaeocystis*, diatoms, and coccolithophores to total chlorophyll in summer are 20% (33%), 68% (64%), and 5% (<1%), respectively, in good agreement with the CHEMTAX climatology (28% (27%), 46% (48%), and 3% (1%), respectively, Fig. 2b & c). Acknowledging the uncertainty in the attribution of the group "Other" in the CHEMTAX data to a model PFT ("Other" includes dinoflagellates, cryptophytes, and chlorophytes, see section 2.3.1), the model also captures the seasonal evolution of the relative importance of *Phaeocystis* and diatoms reasonably well, both averaged over 30-90° S (Fig. 2b) and at high SO latitudes (Fig. 2c-d). The model overestimates the contribution of *Phaeocystis* in fall (39% as compared to 24% in CHEMTAX) and spring (51% as compared to 28%) between 60-90° S and in the Ross Sea, respectively (Fig. 2c-d), but the limited number of data points available in the CHEMTAX climatology in this area and the uncertainty in the attribution of pigments in CHEMTAX to the *Phaeocystis* PFT in ROMS-BEC have to be noted (see section 2.3.1).

In the 4-PFT setup of ROMS-BEC, the simulated summer phytoplankton community south of 60° S was often almost solely composed of diatoms (Fig. S4 and Nissen et al., 2018), suggesting that the implementation of *Phaeocystis* led to a substantial improvement in the representation of the observed high-latitude community structure (Fig. 2). Concurrently, as the distribution of silicic acid and nitrate is directly impacted by the relative importance of silicifying and non-silicifying phytoplankton, such as *Phaeocystis*, in the community, the addition of *Phaeocystis* to the model led to an improvement in the simulated high-latitude nutrient distributions when comparing to climatological data from the World Ocean Atlas (WOA, Fig. S5d-f, Garcia et al., 2014b). Upon the addition of *Phaeocystis*, the zonal average location of the silicate front, i.e., the latitude at which nitrate and silicic acid concentrations are equal (Freeman et al., 2018), is shifted northward by ∼7° C in ROMS-BEC (from 57.1° S in 4-PFT setup to 50° S in 5-PFT setup, see Fig. S6). While this is further north than suggested by WOA data (56.5° S, Fig. S6b and Garcia et al., 2014b), this can certainly be expected to affect the competitive fitness of individual phytoplankton types in the subantarctic and possibly at lower latitudes, which we did not assess further in this study. Overall, our model suggests that *Phaeocystis* is an important member of the high-latitude phytoplankton community. In the remainder of the manuscript, we will therefore explore the temporal variability in the relative importance of diatoms and *Phaeocystis* and its implications for SO carbon cycling in more detail.

3.2 Bloom characteristics & seasonal succession

Maximum total chlorophyll concentrations are simulated for the first half of December across latitudes in ROMS-BEC (solid blue line in Fig. 3a). At high SO latitudes south of 60° S, this is 1-2 months earlier than suggested by satellite estimates (black line in Fig. 3a). Yet, compared to the 4-PFT setup (dashed blue line in Fig. 3a), the simulated timing of peak chlorophyll levels improved in this study, with peak chlorophyll delayed by on average a week in the model upon the implementation of *Phaeocystis*. The simulated physical biases (i.e., generally too high temperatures and too shallow mixed layer depths, both favoring an earlier onset of the phytoplankton bloom, see Nissen et al., 2018) only partially explain the bias in the simulated

https://doi.org/10.5194/bg-2019-488
Preprint. Discussion started: 31 January 2020

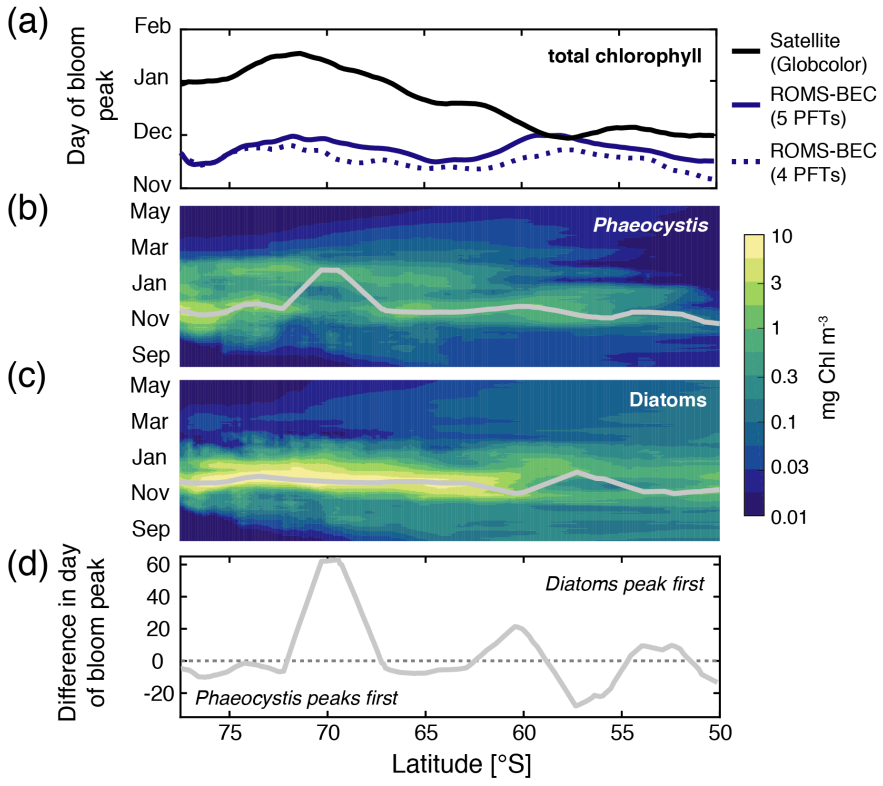

Figure 3. Hovmoller plots south of 50° S of a) the day of maximum total chlorophyll concentrations in a satellite product (black line, Globcolor climatology from 1998-2018 based on the daily 25 km chlorophyll product, see Fanton d'Andon et al., 2009; Maritorena et al., 2010), the *Baseline* simulation of this study (solid blue line), and the *Baseline* simulation of Nissen et al. (2018, dashed blue line; without *Phaeocystis*), and daily surface b) diatom and c) *Phaeocystis* chlorophyll biomass concentrations [mg chl m^{-3}]. Overlain are the average day of the peak concentrations for each latitude (see also section 2.3.1). Panel d) denotes the difference in days in the timing of the bloom peak of diatoms and *Phaeocystis* for each latitude, with negative values denoting a succession from *Phaeocystis* to diatoms throughout the season.

timing of maximum chlorophyll levels (see red and green dashed lines in Fig. S7a), suggesting that biological factors must explain the difference between ROMS-BEC and the satellite product. As diatoms dominate the phytoplankton community at peak total chlorophyll concentrations everywhere in the model domain (compare their bloom timing in Fig. 3c to Fig. 3a and to the simulated community composition in Fig. 2b-d), the mismatch in timing is likely related to the representation of this PFT in the model, and is possibly at least partly caused by their comparatively high growth rates at low temperatures (see Fig. A1a).

In contrast to diatoms, maximum chlorophyll concentrations of *Phaeocystis* are simulated for late November or early December across most latitudes in the model (only around 70° S a peak in late January is simulated, Fig. 3b). Overall, the timing of simulated peak *Phaeocystis* chlorophyll levels corresponds well to the suggested timing of observed maximum seawater DMSP concentrations (peak in November/December in Curran et al., 1998; Curran and Jones, 2000) and the delayed maximum atmospheric DMS concentrations (January/February, e.g. Nguyen et al., 1990; Ayers et al., 1991). This further corroborates the

https://doi.org/10.5194/bg-2019-488
Preprint. Discussion started: 31 January 2020

Biogeosciences
Discussions
Open Access
EGU

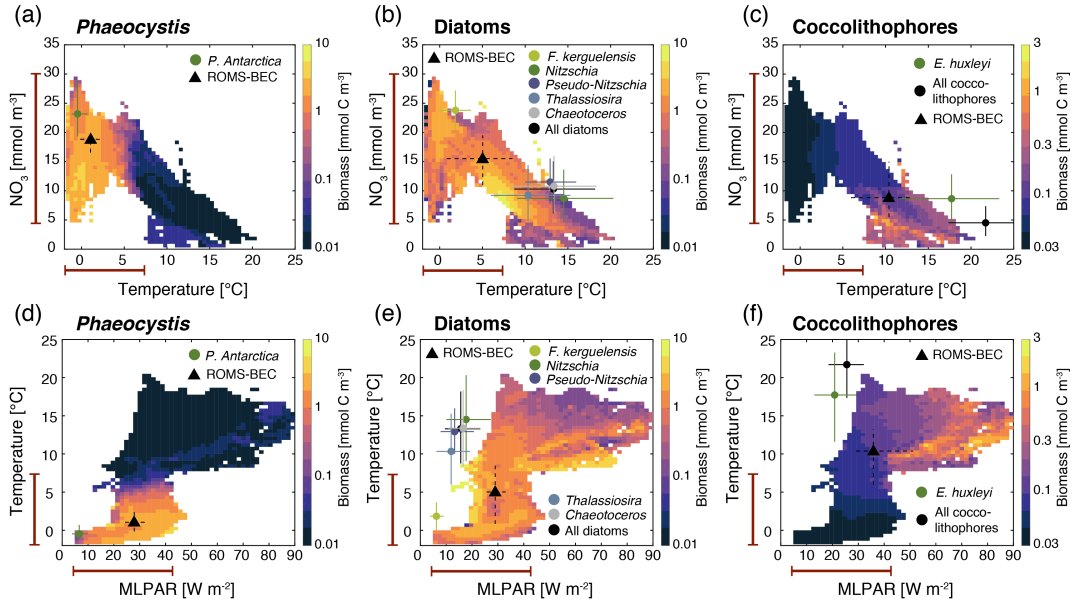

Figure 4. Simulated DJFM average top 50 m average a) & d) *Phaeocystis*, b) & e) diatom, and c) & f) coccolithophore carbon biomass concentrations [mmol C m^{-3}] south of 40° S as a function of the simulated concurrent a)-c) nitrate concentrations [mmol N m^{-3}] and temperature (° C) and d)-f) temperature [° C] and mixed layer PAR levels (W m^{-2}). Overlain are the observed ecological niche centers (median) and breadths (inter quartile ranges) for example taxa of the three functional types from Brun et al. (2015, circles and solid lines) and as simulated in ROMS-BEC (triangles and dashed lines; area and biomass weighted). The red bars on the axes indicate the simulated range of the respective environmental condition in ROMS-BEC between 60-90° S and averaged over DJFM and the top 50 m.

hypothesis that the bias in the timing of maximum total chlorophyll levels in ROMS-BEC is likely caused by how diatoms are parameterized in the model. Taken together, the model simulates a succession from *Phaeocystis* to diatoms close to the Antarctic continent (south of 72° S, see also Fig. S7b) and in some parts of the open ocean north of 68° S (Fig. 3d & Fig. S7b). The difference in the timing of the bloom peak between the two PFTs is largely <10 days when averaged zonally, but locally exceeds 30 days when looking at individual grid cells in the model (Fig. S7b), in broad agreement with observations, which suggest up to 2 months between the peak chlorophyll concentrations of *Phaeocystis* and diatoms in the Ross Sea (see e.g. Peloquin and Smith, 2007; Smith et al., 2011). Subsequently, we will assess how environmental conditions and biomass loss processes interact to control the SO phytoplankton biogeography and in particular the competition between *Phaeocystis* and diatoms at high SO latitudes.

3.3 Analyzing ecological niches: A bottom-up perspective on SO phytoplankton biogeography

Relating the observed or simulated biomass concentrations of a PFT to the concurrent environmental conditions allows for an assessment of the ecological niche of the PFT in question. In ROMS-BEC, in agreement with their distinct simulated geographical distributions in summer (Fig. 1c-e), *Phaeocystis*, diatoms, and coccolithophores also occupy distinct ecological

https://doi.org/10.5194/bg-2019-488
Preprint. Discussion started: 31 January 2020

niches in the model. Between 40-90° S, the niche center of DJFM average *Phaeocystis* biomass is simulated at a nitrate concentration of 18.8 mmol m^{-3} (inter quartile range 16.6-20.6 mmol m^{-3}), a temperature of 1.1° C (-0.2-2.6° C), and MLPAR of 27.8 W m^{-2} (24.3-32 W m^{-2}, Fig. 4a & d). In comparison, diatoms occupy a wider niche in temperature (inter quartile range 0.8-8.5° C, niche center at 5° C, Fig. 4b). While the niche center is at lower nitrate concentrations for diatoms (15.5 mmol m^{-3}) than for *Phaeocystis* (18.8 mmol m^{-3}), maximum diatom biomass at high SO latitudes, i.e., where DJFM average temperatures are <5° C, is simulated at higher nitrate concentrations than maximum *Phaeocystis* biomass (Fig. 4a & b). In the model, averaged over the summer, the difference in biomass concentrations across MLPAR between diatoms and *Phaeocystis* is rather small (niche center at 28.9 W m^{-2} and 27.8 W m^{-2}, respectively, Fig. 4d & e). In agreement with their maximum simulated biomass concentrations in the subantarctic (section 3.1), the niche center of coccolithophore biomass is at higher temperatures (10.4° C), higher light levels (35.8 W m^{-2}), and lower nitrate concentrations (8.8 mmol m^{-3}) than the niche center of the other two PFTs (Fig. 4c & f). Regarding iron, the three PFTs do not occupy distinct ecological niches in ROMS-BEC (niche centers at 0.32 μmol m^{-3}, 0.32 μmol m^{-3}, and 0.34 μmol m^{-3} for *Phaeocystis*, diatoms, and coccolithophores, respectively, see Fig. S8). Given that phytoplankton growth is limited by iron availability in the high-latitude SO in the model (Fig. S1), this suggests that the spatio-temporal averaging applied here potentially precludes the assessment of the ecological niche in iron space (by averaging over DJFM here if iron were to matter on a sub-seasonal scale).

In comparison to the ecological niches of important SO phytoplankton taxa derived by Brun et al. (2015) based on global presence/absence observations of phytoplankton and species distribution models, the niche centers of all PFTs are simulated at higher MLPAR in the model (∼30 W m^{-2}, ∼30 W m^{-2}, and ∼35 W m^{-2}) than in available observations (∼10 W m^{-2}, ∼20 W m^{-2} and ∼30 W m^{-2} for *Phaeocystis*, diatoms, and coccolithophores, respectively, Fig. 4d-f). Yet, the 5-20 W m^{-2} higher model-based estimates are consistent with the mixed layer depth bias in ROMS-BEC (see Nissen et al., 2018). While the simulated niche of diatoms regarding temperature and nitrate is in broad agreement with that observed for example SO taxa (Fig. 4b), the simulated niches are wider for *Phaeocystis* (Fig. 4a) and generally centered around lower temperatures for coccolithophores (Fig. 4c). Acknowledging the difficulties comparing a model PFT to individual phytoplankton taxa, a sampling bias towards temperate and tropical species/strains, and the overall low data coverage in the high-latitude SO, we conclude that the simulated ecological niches of *Phaeocystis*, diatoms, and coccolithophores are largely in agreement with available observations. Since the analysis of the summer average ecological niches does not inform about sub-seasonal environmental variability and neglects the role of top-down factors in controlling the simulated distributions of phytoplankton types, we will assess these in more detail for the simulated competition between *Phaeocystis* and diatoms in the following.

3.4 High-latitude competition of *Phaeocystis* and diatoms: An assessment of bottom-up and top-down factors

The temporal evolution of the relative growth ratio, i.e., the ratio of the specific growth rates of diatoms and *Phaeocystis* (Eq. 2), informs about the competitive advantage of one PFT over the other throughout the year. In ROMS-BEC, the relative growth ratio is negative throughout spring and fall between 60-90° S (μ^{PA} is on average 5%/6% larger than μ^{D} in spring/fall) and only positive between early December and early February (μ^{D} is on average 5% larger than μ^{PA} in summer, Fig. 5a & c). Hence, bottom-up factors promote the accumulation of *Phaeocystis* (diatom) relative to diatom (*Phaeocystis*) biomass in

https://doi.org/10.5194/bg-2019-488
Preprint. Discussion started: 31 January 2020

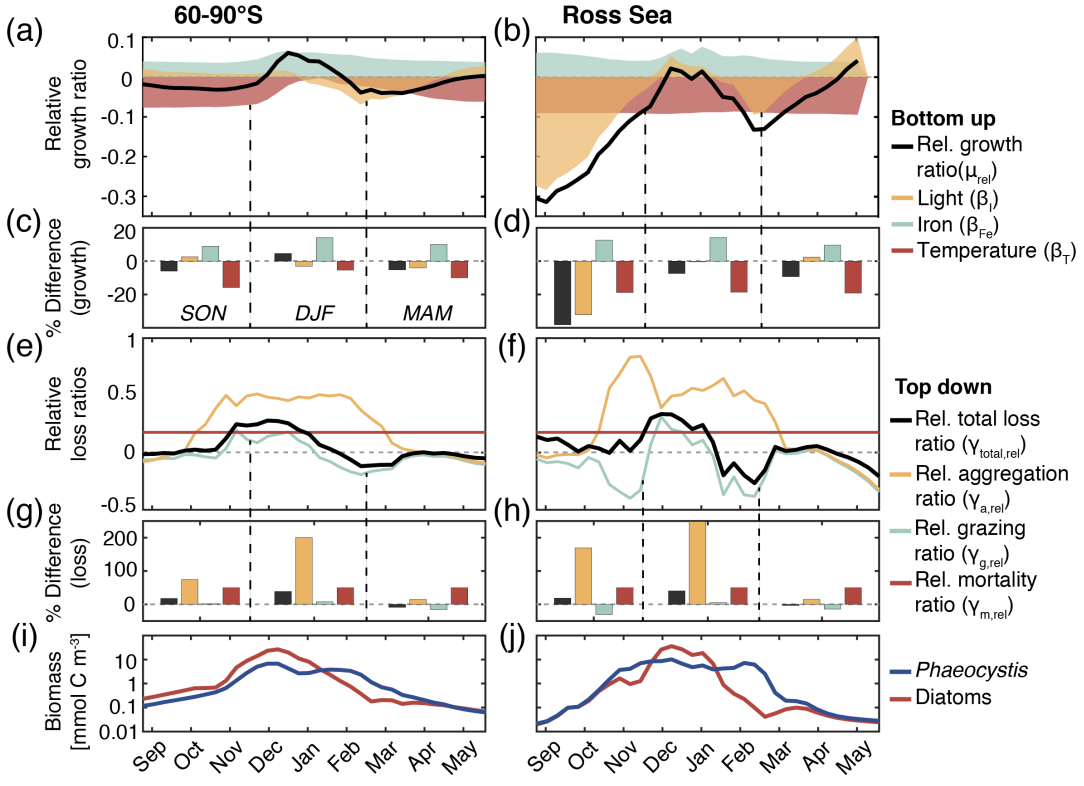

Figure 5. a) & b) Relative growth ratio (black) of diatoms vs. *Phaeocystis*. The colored areas are the contributions of the limitation of growth by light (yellow, β_{I}), iron (blue, β_{Fe}), and temperature (red, β_{T}, see Eq. 2). c) & d) Seasonally averaged percent difference between diatoms and *Phaeocystis* in the specific growth rate (black), light limitation (yellow), iron limitation (blue), and temperature limitation (red). Calculated from non-log-transformed ratios, i.e., e.g. black bar corresponds to $10^{\mu_{\mathrm{rel}}^{\mathrm{DPA}}}$ (see Eq. 2). e) & f) Relative total loss ratio (black) of diatoms vs. *Phaeocystis*, with contributions of the relative grazing ratio (blue), relative non-grazing loss ratio (red), and relative aggregation ratio (yellow, see Eq. 3-6). g) & h) Seasonally averaged percent difference between diatoms and *Phaeocystis* in the total specific loss rate (black), specific aggregation rate (yellow), specific grazing rate (blue), and specific mortality rate (red), calculated from non-log-transformed ratios. i) & j) *Phaeocystis* (blue) and diatom (red) surface carbon biomass concentrations [mmol C m^{-3}]. For all metrics, the left panels are averaged over 60-90° S and those on the right for the Ross Sea.

spring/fall (summer) in this area in our model. In comparison, the relative growth ratio is positive for a shorter time period in the Ross Sea ($\mu^{\mathrm{D}}>\mu^{\mathrm{PA}}$ between mid-December and mid-January, Fig. 5b). In fact, averaged seasonally, the specific growth rate of *Phaeocystis* is larger than that of diatoms for all seasons ($\mu_{\mathrm{rel}}^{\mathrm{DPA}}<0$), being up to 38% larger in spring (Fig. 5d), suggesting that bottom-up factors are particularly favorable for the accumulation of *Phaeocystis* biomass in the Ross Sea.

To understand the controls of the spatio-temporal differences in the specific growth rates, the relative growth ratio can be broken down into the environmental factors contributing to the simulated specific growth rate of each phytoplankton type at any point in time (Eq. 2, colors in Fig. 5a-d). As a direct result of the higher k_{Fe} of *Phaeocystis* in the model (Table 1), the iron

https://doi.org/10.5194/bg-2019-488
Preprint. Discussion started: 31 January 2020


Biogeosciences Discussions Open Access EGU

limitation of their growth is stronger than that of diatoms, and iron availability, i.e., β_{Fe} in Eq. 2, is an advantage for diatoms both between 60-90° S and in the Ross Sea at all times (blue area is positive, up to 14% stronger iron limitation of *Phaeocystis* in both areas in summer, see Fig. 5a-d). Yet, the two subareas differ in the simulated temperature and light limitation of growth of *Phaeocystis* and diatoms. Overall, temperature is limiting diatom growth more than *Phaeocystis* growth in both subareas throughout the year (β_{T}<0; up to 16% and 19% stronger growth limitation between 60-90° S and in the Ross Sea, respectively, see red areas in Fig. 5a-d). While the growth advantage of *Phaeocystis* regarding temperature is rather constant over time in the Ross Sea (Fig. 5b & d), their advantage is substantially smaller in summer between 60-90° S (5%, Fig. 5a & c). Additionally, the difference in light limitation between diatoms and *Phaeocystis* is rather small in this area (3-4% throughout the year, yellow areas in Fig. 5a & c), implying that their differences in α_{PI} (Table 1) are balanced by differences in photoacclimation in ROMS-BEC (Geider et al., 1998; Nissen et al., 2018). Consequently, the combination of the comparatively large advantage in iron limitation and the rather small disadvantage in temperature limitation results in the higher specific growth rates of diatoms in summer between 60-90° S. In contrast, in the Ross Sea, differences in light limitation between diatoms and *Phaeocystis* are large, with a maximum advantage for *Phaeocystis* in spring (their growth is 32% less light limited; Fig. 5b & d). Therefore, the difference in light limitation predominantly controls the seasonality of the relative growth ratio (Fig. 5b) and promotes the dominance of *Phaeocystis* over diatoms early in the growing season in this area in our model (Fig. 5j), which is not simulated when averaging over 60-90° S (Fig. 5i). Altogether, in ROMS-BEC, differences in growth between diatoms and *Phaeocystis* are mostly controlled by seasonal differences in iron/temperature (60-90° S) and iron/light conditions (Ross Sea), respectively. Still, given the simulated growth advantage of *Phaeocystis* throughout much of the growing season in both subareas, bottom-up factors alone cannot explain why *Phaeocystis* only dominates over diatoms temporarily (Fig. 5i & j), implying that top-down factors need to be considered to explain their biomass evolution in our model.

In both subareas, the simulated relative total loss ratio is positive throughout spring and summer, implying that the specific total loss rate of *Phaeocystis* is higher than that of diatoms ($\gamma^{\mathrm{PA}}_{\mathrm{total}}$>$\gamma^{\mathrm{D}}_{\mathrm{total}}$, see Eq. 6), which favors the accumulation of diatom biomass relative to that of *Phaeocystis* (Fig. 5e-h). In fact, the total loss rate of *Phaeocystis* is on average 17%/38% (60-90° S) and 18%/40% (Ross Sea) higher than that of diatoms in spring/summer in ROMS-BEC (Fig. 5g & h). In the model, the relative total loss ratio is only negative in early fall in both subareas ($\gamma^{\mathrm{D}}_{\mathrm{total}}$>$\gamma^{\mathrm{PA}}_{\mathrm{total}}$, Fig. 5e & f), but in this season, the difference between diatoms and *Phaeocystis* in their specific total loss rates is overall smaller than in the other seasons (9% and 3% between 60-90° S and in the Ross Sea, respectively, Fig. 5g & h). The simulated seasonality of the total loss ratio is the result of the interplay between losses through grazing, aggregation, and non-grazing mortality of each phytoplankton type in ROMS-BEC (Eq. 6, colors in Fig. 5e-h). Of all three loss pathways, differences in aggregation losses are largest between *Phaeocystis* and diatoms both between 60-90° S (up to 200% higher aggregation losses for *Phaeocystis* in summer, yellow in Fig. 5e & g) and in the Ross Sea (up to 250% higher in summer, Fig. 5f & h). In comparison, differences between *Phaeocystis* and diatoms in grazing (up to 16% and 14% between 60-90° S and in the Ross Sea, respectively) and mortality losses (50% everywhere) are considerably smaller (see blue and red areas in Fig. 5e-h, respectively), suggesting that aggregation losses predominantly contribute to the simulated differences in the total loss rates between *Phaeocystis* and diatoms.

https://doi.org/10.5194/bg-2019-488
Preprint. Discussion started: 31 January 2020

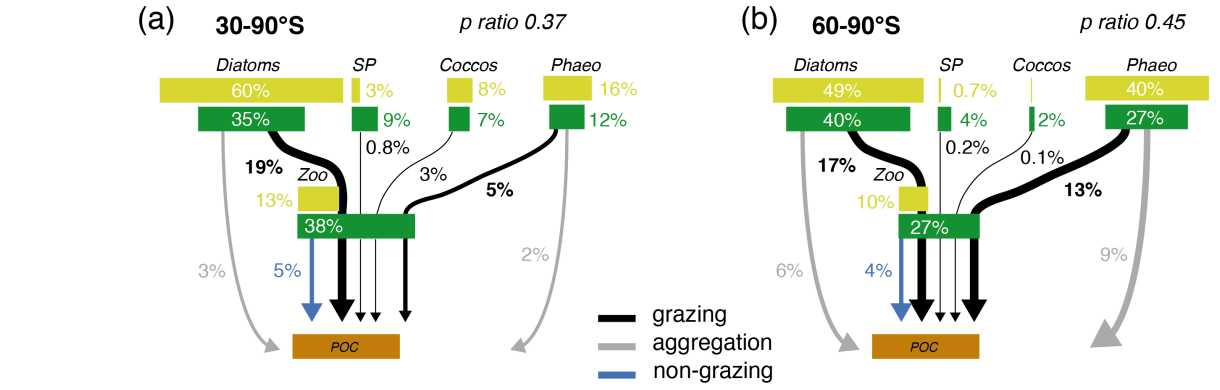

Figure 6. Pathways of particulate organic carbon (POC) formation in the *Baseline* simulation of ROMS-BEC averaged annually over a) 30-90° S and b) 60-90° S. The green and yellow boxes show the relative contribution (%) of *Phaeocystis*, diatoms, coccolithophores, small phytoplankton (SP), and zooplankton (Zoo) to the combined phytoplankton and zooplankton biomass (green) and total POC production (yellow) in the top 100 m, respectively. The arrows denote the relative contribution of the different POC production pathways associated with each PFT (black = grazing by zooplankton, grey = aggregation, blue = non-grazing mortality), given as % of total NPP in the top 100 m. Numbers are printed if ≥0.1% and rounded to the nearest integer if >0.5%. The sum of all arrows gives the POC production efficiency (p ratio). Note that diazotrophs are not included in this figure due to their minor contribution to NPP in the model domain.

In summary, between 60-90° S, the simulated growth advantage of *Phaeocystis* early in the season (facilitated by advantages in the temperature limitation of their growth) are not large enough to outweigh the disadvantages in iron limitation of their growth and in the biomass losses they experience. As a result, in spring and summer, *Phaeocystis* do not accumulate substantial biomass relative to (or even dominate over) diatoms in this subarea in ROMS-BEC. In the Ross Sea, however, the simulated growth advantages of *Phaeocystis* (resulting from advantages in the light and temperature limitation of their growth) are large enough to outweigh the disadvantages in iron limitation and specific biomass loss rates, allowing them to dominate over diatoms early in the growing season in our model and explaining the simulated succession from *Phaeocystis* to diatoms close to the Antarctic continent (see also section 3.2). Ultimately, this simulated spatio-temporal variability in the relative importance of *Phaeocystis* and diatoms has implications for both SO and global carbon cycling, which we will assess subsequently.

3.5 Quantifying the importance of *Phaeocystis* for the cycling of carbon

Phaeocystis is an important member of the SO phytoplankton community in our model, particularly south of 60°S, where it contributes 46% and 40% to total annual NPP and POC formation, respectively. (Table 3 & Fig. 6). Even when considering the entire region south of 30°S, the contribution of *Phaeocystis* to NPP (15%) and POC production (16%) is sizeable. The simulated spatial differences in phytoplankton community structure have direct implications for the fate of organic carbon upon biomass loss, and Fig. 6 illustrates the different pathways of POC formation for each PFT in ROMS-BEC. Overall, in our model, the p ratio, i.e., the fraction of NPP that is transformed to sinking POC (Laufkötter et al., 2016), is higher at high latitudes south of 60° S (45%) than the domain average (37%, Fig. 6). This is a direct result of the higher fraction of large phytoplankton

https://doi.org/10.5194/bg-2019-488
Preprint. Discussion started: 31 January 2020

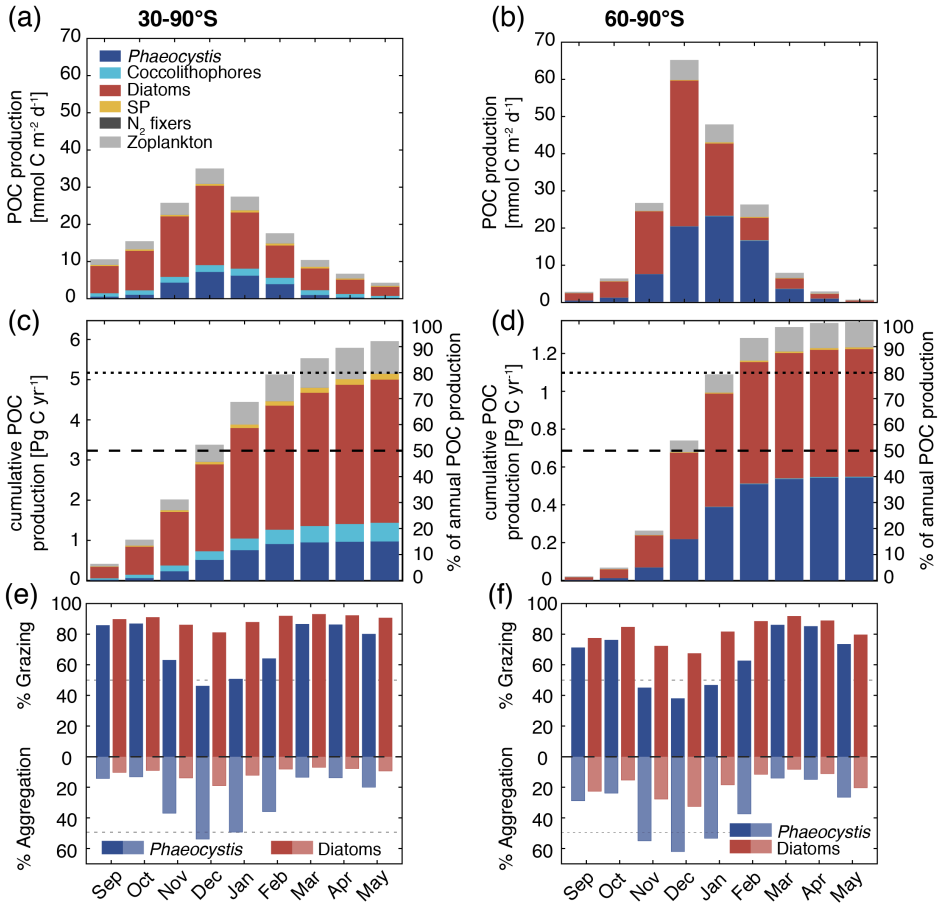

Figure 7. Simulated vertically integrated production of particulate organic carbon (POC) a) & b) as a function of time [mmol C m^{-2} d^{-1}], c) & d) cumulative over time (absolute production in Pg C yr^{-1} on the left axis and relative to annually integrated production on the right axis), and e) & f) as a function of time via grazing and aggregation, respectively. The colors correspond to the different PFTs in ROMS-BEC, and the panels correspond to averages or integrals over 30-90° S (left) and 60-90° S (right), respectively.

types, i.e., *Phaeocystis* and diatoms, in the phytoplankton community in this area (Fig. 2), facilitating more carbon export relative to NPP in the model. In fact, our model results suggest that these two large phytoplankton types contribute more to POC formation than to total biomass (compare yellow and green boxes in Fig. 6). Integrated annually, diatoms contribute most of all PFTs to POC formation in our model (60% and 49% between 30-90° S and 60-90° S, respectively, Fig. 6). For both diatoms and *Phaeocystis*, grazing by zooplankton (i.e., the formation of fecal pellets) is the most important pathway of POC production in ROMS-BEC (black arrows in Fig. 6, 13%/52% and 29%/37% of total POC production for *Phaeocystis*/diatoms between 30-90° S and 60-90° S, respectively). Yet, at high latitudes (60-90° S), aggregation of *Phaeocystis* biomass contributes significantly to POC formation (20% of total POC production, 9% of NPP, grey arrows in Fig. 6b). Given that the loss of biomass via a given pathway is a function of the local biomass concentrations of each PFT at any given point in time (see

https://doi.org/10.5194/bg-2019-488
Preprint. Discussion started: 31 January 2020

section 2.1 and Nissen et al., 2018), the relative importance of any PFT or biomass loss pathway for total POC formation and hence the total POC produced vary throughout the year.

The seasonal variability in total POC formation is governed by the variability in total chlorophyll concentrations both between 30-90° S and 60-90° S, and peak POC formation rates of 35 mmol m^{-2} d^{-1} (30-90° S) and 65 mmol m^{-2} d^{-1} (60-90° S) are simulated for December in ROMS-BEC (Fig. 7a & b; compare to Fig. 3a). Similarly, the contribution of *Phaeocystis* and diatoms to total POC formation closely follows their contribution to total biomass over the year, with the contribution of *Phaeocystis* peaking in January (23%) and February (63%) for 30-90° S and 60-90° S, respectively (Fig. 7a & b; compare timing to Fig. 2b & c). As a result of the close link between POC formation and chlorophyll concentrations in ROMS-BEC, the majority of the annual POC formation occurs between November and February in our model (64% and 88% south of 30° S and 60° S, respectively, Fig. 7c & d). During these months, the simulated pathways of POC formation differ from the annually integrated perspective in Fig. 6, especially for *Phaeocystis*. While grazing is the most important pathway throughout the year for diatoms in both subareas in our model (red bars in Fig. 7e & f), aggregation of *Phaeocystis* is as important as grazing in December and January between 30-90° S (blue bars in Fig. 7e) and even dominantly contributes to POC formation between November and January at high SO latitudes (up to 65%, blue bars in Fig. 7f). Altogether, this implies that both spatial and temporal variations in SO phytoplankton community structure critically impact the fate of carbon beyond the upper ocean.

4 Discussion

4.1 Biogeochemical implications of SO *Phaeocystis* biogeography

Our simulated contribution of *Phaeocystis* to SO NPP and net POC formation is higher than that found in the previous modeling study by Wang and Moore (2011), particularly at higher latitudes: They diagnosed a contribution of 13% and 23% to NPP south of 40° S and 60° S, respectively, compared to our estimates of 15% for south of 30° S and 46% for the region south of 60° S. We interpret the difference to stem primarily from differences in parameter choices of the PFTs between the two models. As an example, the half-saturation constant of iron of *Phaeocystis* is 125% larger than that of diatoms in the model by Wang and Moore (2011, 0.18 μmol m^{-3} for *Phaeocystis* as compared to 0.08 μmol m^{-3} for diatoms), but only 33% larger in ours (Table 1). The resulting smaller difference in the growth limitation by iron in ROMS-BEC leads to more competitive *Phaeocystis* relative to diatoms in the iron-depleted SO and can at least partially explain the higher relative importance of *Phaeocystis* in our model. In fact, differences in model parameters between *Phaeocystis* and diatoms in ROMS-BEC can alter the simulated contribution of *Phaeocystis* to total NPP from 5-32% and 17-63% between 30-90° S and 60-90° S, respectively (see section A1, as well as section 2.2 and Table 2). This illustrates how single model parameters sensitively impact the competitive success of *Phaeocystis* in the SO. Still, the simulated community structure in the *Baseline* simulation with ROMS-BEC is supported by available observations (see section 3.1), giving us confidence in our estimates.

The simulated contribution of *Phaeocystis* to POC export in ROMS-BEC (16% and 40% south of 30° S and 60° S) is in broad agreement with the previous estimate from Wang and Moore (2011, 19% and 30% south of 40° S and 60° S, respectively). This is despite the differences in phytoplankton community structure between the two models (see above) and demonstrates our on-

https://doi.org/10.5194/bg-2019-488
Preprint. Discussion started: 31 January 2020

going limited quantitative understanding of the fate of biomass losses (see also Laufkötter et al., 2016). Across the parameter sensitivity runs in ROMS-BEC (section 2.2), the contribution of *Phaeocystis* to POC production and export varies from 4-23% and 13-59% south of 30° S and 60° S, respectively. In addition to this uncertainty resulting only from the growth and loss parameters of *Phaeocystis* in the model (Table 2), further uncertainty arises from parameters describing the partitioning of biomass losses amongst dissolved and particulate carbon species, which we did not assess in this study. Acknowledging that the exact numbers are highly sensitive to parameter choices in the model, our analysis reveals how the pathways of POC production, in particular the relative importance of fecal pellets from zooplankton and aggregated phytoplankton cells, are impacted by the simulated spatio-temporal variability in phytoplankton community structure throughout the year (Fig. 7). In this regard, the simulated strong temporal coupling between POC fluxes and biomass distributions in ROMS-BEC is a direct result of the model formulations describing particle sinking (Lima et al., 2014). This coupling is supported by observations, e.g., from the Ross Sea, where the POC flux from the upper ocean has been found to be closely linked to biomass levels in the overlying surface layer (with aggregates being an important vector for POC export when *Phaeocystis* dominated the community, Asper and Smith, 1999). Yet, the coupling in our model is potentially too strong in other areas, where reprocessing of POC by zooplankton in the upper ocean or lateral advection of POC could decouple the seasonal evolution of phytoplankton biomass and POC export (e.g. Lam and Bishop, 2007; Stange et al., 2017), the effect of which we can currently not assess. Given the possibly large importance of different POC production pathways for carbon and nutrient cycling through their impact on the remineralization depth of organic matter, these processes should be better constrained in the future, in order to further quantify the imprint of spatio-temporal variations in the relative importance of *Phaeocystis* for the high-latitude cycling of carbon. Despite these uncertainties, *Phaeocystis* is clearly a substantial player on the global scale. Comparing the model-simulated integrated NPP and POC export across the entire model domain with data-based estimates of global NPP and POC export suggests that SO *Phaeocystis* alone contribute about 5% to globally integrated NPP (58±7 Pg C yr^{-1}, Buitenhuis et al., 2013a), and about the same percentage to global POC export (9.1±0.2 Pg C yr^{-1}, DeVries and Weber, 2017).

Besides its impact on the carbon cycle, *Phaeocystis* is the major contributor to the marine sulphur cycle in the SO through its production of DMSP (Keller et al., 1989; Liss et al., 1994; Stefels et al., 2007). Integrating the modeled *Phaeocystis* biomass loss rates via zooplankton grazing and non-grazing mortality and making assumptions regarding the corresponding DMS(P) release (see scetion 2.3.1), our estimated annual DMS production by *Phaeocystis* in ROMS-BEC amounts to 3.3-11.5 Tg S and 1.8-6.4 Tg S south of 30° S and 60° S, respectively. Consequently, assuming that all of this DMS production quickly escapes to the atmosphere, our estimates correspond to 11.6-40.1% (30-90° S) and 6.5-22.7% (60-90° S) of the global flux of DMS to the atmosphere previously estimated by Lana et al. (2011, 28.1 Tg S yr^{-1}). Our estimate is an upper bound, however, as not all DMS produced in seawater is readily released to the atmosphere. In fact, a fraction is likely broken down by bacteria, by photolysis, or is mixed down in the water column (see e.g. Simó and Pedrós-Alló, 1999; Stefels et al., 2007). Still, given that other phytoplankton types also produce DMS(P) (Keller et al., 1989; Stefels et al., 2007), the ROMS-BEC-based contribution of SO *Phaeocystis* alone (3.3-11.5 Tg S yr^{-1}) to the global flux of DMS to the atmosphere is in agreement with the flux suggested in Lana et al. (2011, 8.1 Tg S yr^{-1} south of 30° S, i.e., 29% of their global estimate), and the substantial contribution of SO *Phaeocystis* underpins its major role for the global cycling of sulphur.

https://doi.org/10.5194/bg-2019-488
Preprint. Discussion started: 31 January 2020

4.2 Drivers of SO *Phaeocystis* biogeography and their competition with diatoms

In ROMS-BEC, the interplay of iron availability with temperature (60-90° S) and light levels (Ross Sea), respectively, largely controls the competitive fitness of *Phaeocystis* relative to diatoms in the high-latitude SO. Yet, differences in the simulated biomass loss rates between the two PFTs (in particular via aggregation) need to be considered in order to explain why peak *Phaeocystis* biomass levels precede those of diatoms only close to the Antarctic continent in the model. In the literature, the spatial distribution of *Phaeocystis* and diatoms and the temporal succession from *Phaeocystis* to diatoms is almost exclusively discussed in terms of light and iron availability (see e.g. Arrigo et al., 1999; Smith et al., 2014). In this context, regions/times of low light and/or high mixed layer depth are typically associated with high *Phaeocystis* abundance (Alvain et al., 2008; Smith et al., 2014), explaining their bloom in spring, whereas iron availability has been suggested to largely control the magnitude of the summer diatom bloom (Peloquin and Smith, 2007; Smith et al., 2011). This is in agreement with the simulated dynamics and parameters chosen in ROMS-BEC, in which the difference in light limitation between growth of *Phaeocystis* and diatoms facilitates early *Phaeocystis* blooms in the Ross Sea. Yet, it has to be noted that advantages in temperature limitation contribute to the growth advantage of *Phaeocystis* in the high-latitude SO in ROMS-BEC as well. Currently, this growth advantage of *Phaeocystis* at temperatures <4° C is possibly underestimated in the model, as diatom growth at low temperatures is currently overestimated when comparing to available laboratory measurements (Fig. A1a). Nevertheless, in agreement with Peloquin and Smith (2007) and Smith et al. (2011), when diatoms reach peak chlorophyll levels in summer in our model, the simulated difference in iron limitation between the two PFTs is largest across the high-latitude SO (Fig. 5a & b), suggesting that any change in summer iron availability will indeed strongly impact peak diatom and hence total chlorophyll levels in ROMS-BEC.

Still, an important limitation in the assessment of the role of iron in controlling the relative importance of *Phaeocystis* in the high-latitude phytoplankton community is the assumption of a constant k_{Fe} of *Phaeocystis* in the model (0.2 μmol m^{-3}, Table 1). In laboratory experiments, the affinity of *Phaeocystis* for iron has been shown to be sensitive to light (Garcia et al., 2009), which is not accounted for in the *Baseline* simulation of ROMS-BEC. In order to assess the possible effect of a varying k_{Fe} on the competition between *Phaeocystis* and diatoms, we fit a polynomial function to describe the k_{Fe} of *Phaeocystis* as a function of the light level (VARYING_kFE simulation in Table 2, Fig. A1b, Garcia et al., 2009). Acknowledging the substantial uncertainty in the fit, our model simulates k_{Fe} <0.2 μmol m^{-3} and even k_{Fe} <0.15 μmol m^{-3} (corresponding to the k_{Fe} of diatoms in the *Baseline* simulation) only at highest light intensities in summer and mostly close to the surface, and 0.2 μmol m^{-3} < $k_{Fe} \leq$ 0.26 μmol m^{-3} elsewhere as a result of low light levels (Fig. S9a & b). While the contribution of *Phaeocystis* to total NPP is only affected to a lesser extent as a consequence (37% and 13% south of 60° S and 30° S, respectively, instead of 46% and 15% in the *Baseline* simulation), the simulated phytoplankton seasonality is impacted substantially. The maximum chlorophyll levels of diatoms occur earlier than those of *Phaeocystis* in many more places of the SO compared to the *Baseline* simulation, both in coastal areas and in the open ocean (Fig. S9c & d). Thus, in order to include light-iron interactions in future modeling efforts with *Phaeocystis* and to assess their impact on the competition of *Phaeocystis* with diatoms throughout the SO, additional measurements are needed for how k_{Fe} varies as a function of the surrounding light level. Taken together, given the likely lower k_{Fe} of *Phaeocystis* at high-latitude light levels in summer than what we currently assume in ROMS-BEC

https://doi.org/10.5194/bg-2019-488
Preprint. Discussion started: 31 January 2020

(Fig. A1b and Garcia et al., 2009) and given the likely underestimation of their growth advantage in temperature, we probably currently underestimate the competitive advantage in growth of *Phaeocystis* relative to diatoms in the model. However, such a potential underestimation in growth advantage does not automatically mean that the contribution of *Phaeocystis* to the phytoplankton community is underestimated as well. This is because of the important role of biomass loss processes to explain why *Phaeocystis* do not outcompete diatoms everywhere in the high latitudes in ROMS-BEC (Fig. 5). Furthermore, the simulated phytoplankton community structure is in good agreement with available observations (Fig. 2).

Loss processes, such as aggregation and grazing, clearly matter for the competitive advantage of one PFT over another, but these loss processes are generally not well quantified and often not studied with sufficient detail. For example, while the modeling study by Le Quéré et al. (2016) demonstrates the importance of such top-down control for total SO phytoplankton biomass concentrations, an analysis of the impact on phytoplankton community structure is lacking. In fact, in the literature, only few studies discuss the role of top-down factors for the relative importance of *Phaeocystis* and diatoms in the high-latitude SO (Granéli et al., 1993; van Hilst and Smith, 2002). In agreement with our results, aggregation has been suggested to be an important process facilitating high POC export when *Phaeocystis* biomass is high (Asper and Smith, 1999), but to what extent this process significantly contributes to the observed relative importance of *Phaeocystis* and diatoms throughout the year in the high-latitude SO remains largely unknown.

Here, our findings suggest an important role for biomass loss processes in controlling the relative importance of *Phaeocystis* and diatoms in ROMS-BEC, but very little quantitative information exists to constrain model parameters (see section 2.1) or to validate the simulated aggregation, grazing, or non-grazing mortality loss rates of *Phaeocystis* and diatoms over time. Additionally, as discussed in Nissen et al. (2018), the single zooplankton grazer is a major limitation of ROMS-BEC. To what extent accounting implicitly for grazing by higher tropic levels in the non-grazing mortality term makes up for not including more zooplankton PFTs remains unclear. Nevertheless, by changing the overall coupling between phytoplankton and zooplankton and through the distinct grazing preferences of the different zooplankton types, the addition of larger zooplankton grazers would likely change the simulated temporal evolution of *Phaeocystis* and diatom biomass in the model (Le Quéré et al., 2016). Therefore, the above mentioned uncertainties should be addressed by future in situ or laboratory measurements in order to better constrain the simulated biomass loss processes, as our findings suggest these to be necessary to explain the seasonal evolution of the relative importance of *Phaeocystis* and diatoms in the high-latitude SO.

4.3 Limitations & Caveats

Our results may be affected by several shortcomings regarding the parameterization of *Phaeocystis*, in particular the representation of its life cycle, the fate of its biomass losses, and its nutrient uptake stoichiometry. We considered here only colonial *Phaeocystis*, thereby implicitly assuming that a seed population of solitary cells is always available for colony formation. Not including an explicit parameterization for single cells and hence life cycle transitions might substantially impact both the seasonal *Phaeocystis* biomass evolution and the competition with diatoms, as solitary cells have been proposed to require less iron (Veldhuis et al., 1991) and are possibly subject to higher loss rates due to e.g. zooplankton grazing compared to colonies (Smith et al., 2003; Nejstgaard et al., 2007). The transition from solitary to colonial cells is a function of the seed population

https://doi.org/10.5194/bg-2019-488
Preprint. Discussion started: 31 January 2020

and light and nutrient levels (Verity, 2000), and transition models have been applied in SO marine ecosystem models (e.g. Popova et al., 2007; Kaufman et al., 2017). Yet, implementing morphotype transitions of *Phaeocystis* into a basin-wide SO model such as ROMS-BEC is severely hindered by data availability. At the moment, 390 *Phaeocystis* biomass observations are included in the MAREDAT data base south of 30° S, and the distinction between solitary and colonial cells is often difficult (Vogt et al., 2012), impeding the basin-wide model evaluation of both *Phaeocystis* life stages. In addition, colonies of *Phaeocystis* are surrounded by a gelatinous matrix, which contains nutrients and carbon (Schoemann et al., 2005), leading to an underestimation of modeled *Phaeocystis* carbon biomass estimates if not accounting for this mucus (Vogt et al., 2012). In ROMS-BEC, this underestimation is likely small, as <20% of the total *Phaeocystis* biomass is reportedly encorporated into the mucus in the SO (Fig. 9 in Vogt et al., 2012). Nevertheless, through its function as a nutrient storage, the mucus promotes the accumulation of *Phaeocystis* biomass relative to other phytoplankton types when the latter become limited by low nutrient availability. While the gelatinous matrix is additionally thought to prevent grazing, the literature on grazing losses of *Phaeocystis* colonies is non-conclusive (Schoemann et al., 2005). This is possibly a result of the large range of sizes of both *Phaeocystis* and the respective grazers, with smaller zooplankton typically grazing less on *Phaeocystis* colonies than larger zooplankton (see reviews by Schoemann et al., 2005; Nejstgaard et al., 2007). As discussed above, the fate of biomass losses of *Phaeocystis* is still poorly constrained (this applies to all model PFTs, see also Laufkötter et al., 2016). Currently, ROMS-BEC treats POC from all formation pathways equal, i.e., once produced, there is no differentiation between POC originating from diatoms or *Phaeocystis* or from grazing or aggregation. In reality, *Phaeocystis* aggregates might be recycled more readily than those from diatoms. This could reconcile our model results, i.e., the substantial simulated contribution of *Phaeocystis* to POC export at 100 m, with observations which suggest that the contribution of *Phaeocystis* to the POC flux across 200 m is small (<5%, Gowing et al., 2001; Accornero et al., 2003; Reigstad and Wassmann, 2007). Ultimately, the C:P and N:P nutrient uptake ratios by *Phaeocystis* and diatoms are higher (147±26.7 and 19.2±0.61) and lower (94.3±20.1 and 9.67±0.33), respectively (Arrigo et al., 1999, 2000), than those originally suggested by Redfield and currently used in ROMS-BEC (117:16:1 for C:N:P uptake by *Phaeocystis* and diatoms, Anderson and Sarmiento, 1994). Consequently, this suggests that not accounting for the non-Redfield ratios in nutrient uptake by these PFTs leads to an over(under)estimation of carbon fixation per unit of P and hence POC export where/when *Phaeocystis* (diatoms) dominate the phytoplankton community.

5 Conclusions

In this modeling study, we present a thorough assessment of the factors controlling the relative importance of SO *Phaeocystis* and diatoms throughout the year and quantify the implications of the spatio-temporal variability in phytoplankton community structure for POC export. In ROMS-BEC, *Phaeocystis* colonies are an important member of the SO phytoplankton community, contributing 15% (16%) to total annual NPP (POC export) south of 30° S. Moreover, their contribution is threefold higher south of 60° S in our model. Given that our results imply a contribution of approximately 5% of SO *Phaeocystis* colonies to total global NPP and POC export, respectively, we recommend the inclusion of an explicit representation of *Phaeocystis* in ecosystem models of the SO. This will allow for a more realistic representation of the SO phytoplankton community structure,

https://doi.org/10.5194/bg-2019-488
Preprint. Discussion started: 31 January 2020

in particular the relative importance of silicifying diatoms and non-silicifying phytoplankton, which we here find to significantly impact the simulated high-latitude nutrient distributions. A follow-up study with both regional SO and global marine ecosystem models should more closely assess what the impact of this simulated change in the relative concentrations of silicic acid and nitrate in the high-latitude SO is on subantarctic and low latitude phytoplankton dynamics.

On a basin-scale, we find that the competition of *Phaeocystis* and diatoms is controlled by seasonal differences in temperature and iron availability, but that variations in light levels are critical on a local scale, e.g. facilitating early blooms by *Phaeocystis* in the Ross Sea, in agreement with previous studies. Yet, our model suggests that the relative importance of *Phaeocystis* and diatoms over a complete annual cycle is ultimately determined by differences in their biomass loss rates (such as zooplankton grazing and aggregation), which in turn impacts the formation of sinking particles and hence carbon transfer to depth. Despite knowing of the importance of top-down factors for global phytoplankton biomass distributions (Behrenfeld, 2014) and for the formation of sinking particles (e.g. Steinberg and Landry, 2017), model parameters describing the fate of carbon after its fixation during photosynthesis are still surprisingly uncertain (Laufkötter et al., 2016), complicating the assessment of the role of biomass loss processes in regulating global biogeochemical cycles.

Environmental conditions in the SO have changed considerably in the last million years (see e.g. Martínez-García et al., 2014), as well as during the past decades (Constable et al., 2014), and are projected to change further during this century (IPCC, 2014). These changes will impact the competitive fitness of *Phaeocystis* and diatoms (see e.g. Hancock et al., 2018; Boyd, 2019) and hence affect the entire phytoplankton community with likely repercussions for the entire food web (Smetacek et al., 2004). Consequently, based on our results, future laboratory and modeling studies should assess how uncertainties in marine ecosystem models surrounding e.g. the parameterization of the life cycle of *Phaeocystis* and the fate of biomass losses impact the simulated relative importance of this phytoplankton type and carbon transfer to depth at high SO latitudes. Thereby, such studies will allow us to better constrain how potential future changes in the high-latitude phytoplankton community structure impact global biogeochemical cycles.

Data availability. Model data are available upon email request to the first author (cara.nissen@usys.ethz.ch) or in the ETH library archive (available at **XX**, last access: **XX**; **XX**).

Appendix A: Evaluating the simulated phytoplankton dynamics in ROMS-BEC

A1 Sensitivity of *Phaeocystis* biogeography to chosen parameter values

We assess the sensitivity of the simulated annual mean *Phaeocystis* biogeography to parameter choices by performing a set of sensitivity experiments (runs 1-6 in Table 2). Overall, the simulated surface *Phaeocystis* biomass concentrations change by $\gtrapprox$ $\pm$50% for each of the experiments in the high-latitude SO (Fig. A2). Between 60-90° S and in the Ross Sea, the largest increase in *Phaeocystis* biomass concentrations is simulated for AGGREGATION (+112% and +96%, respectively, Fig. A2b & c), whereas the strongest decline is simulated for ALPHA_{PI} (-76% and -87%, respectively, Fig. A2b & c). As a response to changes

https://doi.org/10.5194/bg-2019-488
Preprint. Discussion started: 31 January 2020

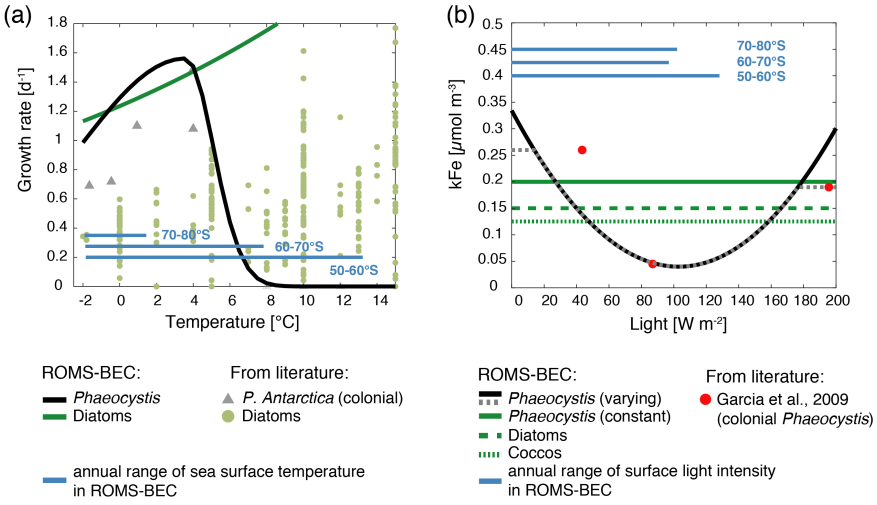

Figure A1. a) Growth rates of *Phaeocystis antarctica* colonies as a function of temperature (conditions of nutrients and light are non-limiting) in laboratory data (grey triangles, see compilation by Schoemann et al., 2005) and as used in ROMS-BEC (black line, see Eq. 1). Green circles and the green line show the temperature-limited growth rate of diatoms in laboratory data (see compilation by Le Quéré et al., 2016) and as used in ROMS-BEC, respectively (see also Table 1). b) Half-saturation constant of Fe (k_{Fe}) of *Phaeocystis* as a function of light intensity I (W m^{-2}) in laboratory data (red circles) and the polynomial fit ($k_{Fe}^{PA}(I) = 2.776 \cdot 10^{-5} \cdot (I + 20)^2$ - $0.00683 \cdot (I + 20) + 0.46$) without (black) and with (dashed grey, as used in ROMS-BEC in simulation VARYING_kFe, see Table 2) the correction at low and high light intensities to restrict k_{Fe} to the range measured in the laboratory experiments by Garcia et al. (2009). The green lines correspond to the half-saturation constants used for *Phaeocystis* (solid), diatoms (dashed), and coccolithophores (dotted) in the *Baseline* simulation in this study (see Table 1). In both panels, the blue lines correspond to the simulated annual range in a) sea surface temperature [° C] and b) light intensity [W m^{-2}] between 50-60° S, 60-70° S, and 70-80° S, respectively.

in *Phaeocystis* parameters, diatom biomass changes overall more than that of SP on a basin scale, suggesting *Phaeocystis* is indeed mostly competing with diatoms for resources in the high-latitude SO. Between 60-90° S, the magnitude of change is similar for the experiments TEMPERATURE (-73%), $ALPHA_{PI}$ (-76%), and IRON (+70%), while in the Ross Sea, the response in IRON is substantially smaller (+17%) than that for the other two experiments (-82% and -87% for TEMPERATURE and $ALPHA_{PI}$, respectively; Fig. A2b & c). This supports our findings from section 3.4, namely that the difference in light sensitivity between *Phaeocystis* and diatoms is more important in coastal areas than on a basin scale in controlling the relative importance of *Phaeocystis* for total phytoplankton biomass.

Author contributions. MV and CN conceived the study. CN set up the model simulations, performed the analysis, and wrote the paper. MV contributed to the interpretation of the results and the writing of the paper.

https://doi.org/10.5194/bg-2019-488
Preprint. Discussion started: 31 January 2020

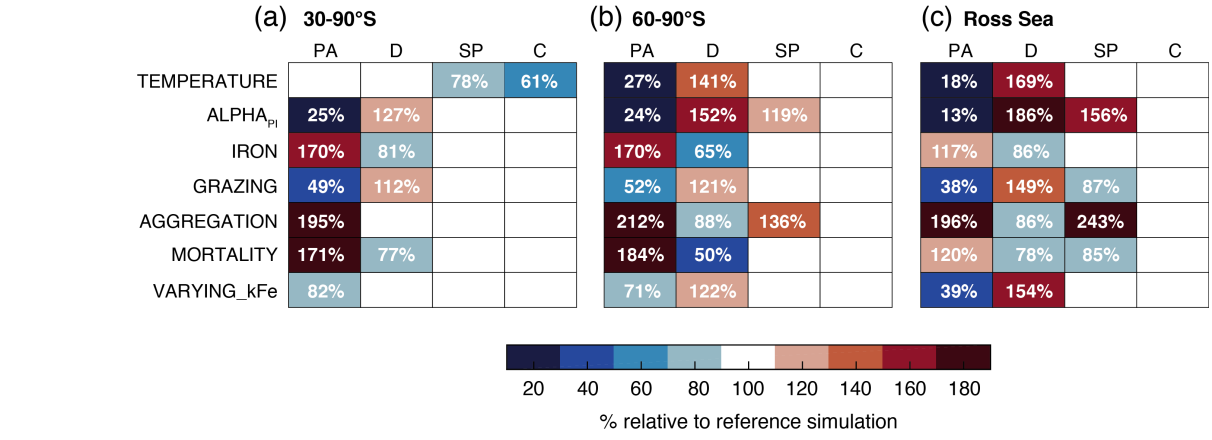

Figure A2. Annual mean surface chlorophyll concentrations of *Phaeocystis* (PA), diatoms (D), small phytoplankton (SP), and coccolithophores (C) in the parameter sensitivity simulations (see section 2.2 and Table 2) relative to the *Baseline* simulation. The model output is averaged over a) 30-90° S, b) 60-90° S, and c) the Ross Sea. Numbers are only printed if the relative change exceeds ±10%

Competing interests. The authors declare that they have no conflict of interest.

Acknowledgements. We acknowledge all the scientists who contributed phytoplankton and zooplankton cell count data to the MAREDAT initiative and William Balch, Helen Smith, Mariem Saavedra-Pellitero, Gustaaf Hallegraeff, José-Abel Flores, and Alex Poulton for providing additional cell count data. Furthermore, GlobColour data (http://globcolour.info) used in this study has been developed, validated, and distributed by ACRI-ST, France. We would like to thank Nicolas Gruber, Matthias Münnich, and Domitille Louchard for valuable discussions and Damian Loher for technical support. Additionally, we would like to thank Gianna Ferrari for the analysis of early ROMS-BEC simulations with *Phaeocystis*. This research was financially supported by the Swiss Federal Institute of Technology Zürich (ETH Zürich) and the Swiss National Science Foundation (project SOGate, grant no. 200021_153452). The simulations were performed at the HPC cluster of ETH Zürich, Euler, which is located in the Swiss Supercomputing Center (CSCS) in Lugano and operated by ETH ITS Scientific IT Services in Zürich. Model output is available upon request to the corresponding author, Cara Nissen (cara.nissen@usys.ethz.ch).

https://doi.org/10.5194/bg-2019-488
Preprint. Discussion started: 31 January 2020

References

Accornero, A., Manno, C., Esposito, F., and Gambi, M. C.: The vertical flux of particulate matter in the polynya of Terra Nova Bay. Part II. Biological components, Antarctic Science, 15, S0954102003001 214, https://doi.org/10.1017/S0954102003001214, 2003.

Alvain, S., Moulin, C., Dandonneau, Y., and Loisel, H.: Seasonal distribution and succession of dominant phytoplankton groups in the global ocean: A satellite view, Global Biogeochemical Cycles, 22, GB3001, https://doi.org/10.1029/2007GB003154, 2008.

Anderson, L. A. and Sarmiento, J. L.: Redfield ratios of remineralization determined by nutrient data analysis, Global Biogeochemical Cycles, 8, 65–80, https://doi.org/10.1029/93GB03318, 1994.

Arrigo, K. R., Weiss, A. M., and Smith, W. O.: Physical forcing of phytoplankton dynamics in the southwestern Ross Sea, Journal of Geophysical Research: Oceans, 103, 1007–1021, https://doi.org/10.1029/97JC02326, 1998.

Arrigo, K. R., Robinson, D. H., Worthen, D. L., Dunbar, R. B., DiTullio, G. R., VanWoert, M. L., and Lizotte, M. P.: Phytoplankton community structure and the drawdown of nutrients and CO_2 in the Southern Ocean, Science, 283, 365–367, https://doi.org/10.1126/science.283.5400.365, 1999.

Arrigo, K. R., DiTullio, G. R., Dunbar, R. B., Robinson, D. H., VanWoert, M., Worthen, D. L., and Lizotte, M. P.: Phytoplankton taxonomic variability in nutrient utilization and primary production in the Ross Sea, Journal of Geophysical Research: Oceans, 105, 8827–8846, https://doi.org/10.1029/1998JC000289, 2000.

Asper, V. L. and Smith, W. O.: Particle fluxes during austral spring and summer in the southern Ross Sea, Antarctica, Journal of Geophysical Research: Oceans, 104, 5345–5359, https://doi.org/10.1029/1998JC900067, 1999.

Ayers, G. P., Ivey, J. P., and Gillett, R. W.: Coherence between seasonal cycles of dimethyl sulphide, methanesulphonate and sulphate in marine air, Nature, 349, 404–406, https://doi.org/10.1038/349404a0, 1991.

Balch, W. M., Bates, N. R., Lam, P. J., Twining, B. S., Rosengard, S. Z., Bowler, B. C., Drapeau, D. T., Garley, R., Lubelczyk, L. C., Mitchell, C., and Rauschenberg, S.: Factors regulating the Great Calcite Belt in the Southern Ocean and its biogeochemical significance, Global Biogeochemical Cycles, 30, 1199–1214, https://doi.org/10.1002/2016GB005414, 2016.

Behrenfeld, M. J.: Climate-mediated dance of the plankton, Nature Climate Change, 4, 880–887, https://doi.org/10.1038/nclimate2349, 2014.

Behrenfeld, M. J. and Falkowski, P. G.: Photosynthetic rates derived from satellite-based chlorophyll concentration, Limnology and Oceanography, 42, 1–20, https://doi.org/10.4319/lo.1997.42.1.0001, 1997.

Berman-Frank, I., Cullen, J. T., Shaked, Y., Sherrell, R. M., and Falkowski, P. G.: Iron availability, cellular iron quotas, and nitrogen fixation in Trichodesmium, Limnology and Oceanography, 46, 1249–1260, https://doi.org/10.4319/lo.2001.46.6.1249, 2001.

Bopp, L., Aumont, O., Cadule, P., Alvain, S., and Gehlen, M.: Response of diatoms distribution to global warming and potential implications: A global model study, Geophysical Research Letters, 32, 1–4, https://doi.org/10.1029/2005GL023653, 2005.

Boyd, P. W.: Physiology and iron modulate diverse responses of diatoms to a warming Southern Ocean, Nature Climate Change, 9, 148–152, https://doi.org/10.1038/s41558-018-0389-1, 2019.

Brun, P., Vogt, M., Payne, M. R., Gruber, N., O'Brien, C. J., Buitenhuis, E. T., Le Quéré, C., Leblanc, K., and Luo, Y.-W.: Ecological niches of open ocean phytoplankton taxa, Limnology and Oceanography, 60, 1020–1038, https://doi.org/10.1002/lno.10074, 2015.

Buitenhuis, E. T., Pangerc, T., Franklin, D. J., Le Quéré, C., and Malin, G.: Growth rates of six coccolithophorid strains as a function of temperature, Limnology and Oceanography, 53, 1181–1185, https://doi.org/10.4319/lo.2008.53.3.1181, 2008.

Buitenhuis, E. T., Hashioka, T., and Le Quéré, C.: Combined constraints on global ocean primary production using observations and models, Global Biogeochemical Cycles, 27, 847–858, https://doi.org/10.1002/gbc.20074, 2013a.

https://doi.org/10.5194/bg-2019-488
Preprint. Discussion started: 31 January 2020

Buitenhuis, E. T., Vogt, M., Moriarty, R., Bednaršek, N., Doney, S. C., Leblanc, K., Le Quéré, C., Luo, Y. W., O'Brien, C., O'Brien, T., Peloquin, J., Schiebel, R., and Swan, C.: MAREDAT: Towards a world atlas of MARine Ecosystem DATa, Earth System Science Data, 5, 227–239, https://doi.org/10.5194/essd-5-227-2013, 2013b.

Buma, A. G. J., Bano, N., Veldhuis, M. J. W., and Kraay, G. W.: Comparison of the pigmentation of two strains of the prymnesiophyte *Phaeocystis* sp., Netherlands Journal of Sea Research, 27, 173–182, https://doi.org/10.1016/0077-7579(91)90010-X, 1991.

Capone, D. G.: Trichodesmium, a Globally Significant Marine Cyanobacterium, Science, 276, 1221–1229, https://doi.org/10.1126/science.276.5316.1221, 1997.

Carton, J. A. and Giese, B. S.: A reanalysis of ocean climate using Simple Ocean Data Assimilation (SODA), Monthly Weather Review, 136, 2999–3017, https://doi.org/10.1175/2007MWR1978.1, 2008.

Chen, Y.-Q., Wang, N., Zhang, P., Zhou, H., and Qu, L.-H.: Molecular evidence identifies bloom-forming *Phaeocystis* (Prymnesiophyta) from coastal waters of southeast China as *Phaeocystis globosa*, Biochemical Systematics and Ecology, 30, 15–22, https://doi.org/10.1016/S0305-1978(01)00054-0, 2002.

Constable, A. J., Melbourne-Thomas, J., Corney, S. P., Arrigo, K. R., Barbraud, C., Barnes, D. K. A., Bindoff, N. L., Boyd, P. W., Brandt, A., Costa, D. P., Davidson, A. T., Ducklow, H. W., Emmerson, L., Fukuchi, M., Gutt, J., Hindell, M. A., Hofmann, E. E., Hosie, G. W., Iida, T., Jacob, S., Johnston, N. M., Kawaguchi, S., Kokubun, N., Koubbi, P., Lea, M.-A., Makhado, A., Massom, R. A., Meiners, K., Meredith, M. P., Murphy, E. J., Nicol, S., Reid, K., Richerson, K., Riddle, M. J., Rintoul, S. R., Smith, W. O., Southwell, C., Stark, J. S., Sumner, M., Swadling, K. M., Takahashi, K. T., Trathan, P. N., Welsford, D. C., Weimerskirch, H., Westwood, K. J., Wienecke, B. C., Wolf-Gladrow, D., Wright, S. W., Xavier, J. C., and Ziegler, P.: Climate change and Southern Ocean ecosystems I: how changes in physical habitats directly affect marine biota, Global Change Biology, 20, 3004–3025, https://doi.org/10.1111/gcb.12623, 2014.

Cubillos, J. C., Wright, S. W., Nash, G., de Salas, M. F., Griffiths, B., Tilbrook, B., Poisson, A., and Hallegraeff, G. M.: Calcification morphotypes of the coccolithophorid *Emiliania huxleyi* in the Southern Ocean: changes in 2001 to 2006 compared to historical data, Marine Ecology Progress Series, 348, 47–54, https://doi.org/10.3354/meps07058, 2007.

Curran, M. A. J. and Jones, G. B.: Dimethyl sulfide in the Southern Ocean: Seasonality and flux, Journal of Geophysical Research: Atmospheres, 105, 20 451–20 459, https://doi.org/10.1029/2000JD900176, 2000.

Curran, M. A. J., Jones, G. B., and Burton, H.: Spatial distribution of dimethylsulfide and dimethylsulfoniopropionate in the Australasian sector of the Southern Ocean, Journal of Geophysical Research: Atmospheres, 103, 16 677–16 689, https://doi.org/10.1029/97JD03453, 1998.

Dee, D. P., Uppala, S. M., Simmons, A. J., Berrisford, P., Poli, P., Kobayashi, S., Andrae, U., Balmaseda, M. A., Balsamo, G., Bauer, P., Bechtold, P., Beljaars, A. C. M., van de Berg, L., Bidlot, J., Bormann, N., Delsol, C., Dragani, R., Fuentes, M., Geer, A. J., Haimberger, L., Healy, S. B., Hersbach, H., Hólm, E. V., Isaksen, L., Kållberg, P., Köhler, M., Matricardi, M., McNally, A. P., Monge-Sanz, B. M., Morcrette, J.-J., Park, B.-K., Peubey, C., de Rosnay, P., Tavolato, C., Thépaut, J.-N., and Vitart, F.: The ERA-Interim reanalysis: configuration and performance of the data assimilation system, Quarterly Journal of the Royal Meteorological Society, 137, 553–597, https://doi.org/10.1002/qj.828, 2011.

Deppeler, S. L. and Davidson, A. T.: Southern Ocean phytoplankton in a changing climate, Frontiers in Marine Science, 4, 40, https://doi.org/10.3389/fmars.2017.00040, 2017.

DeVries, T. and Weber, T.: The export and fate of organic matter in the ocean: New constraints from combining satellite and oceanographic tracer observations, Global Biogeochemical Cycles, 31, 535–555, https://doi.org/10.1002/2016GB005551, 2017.

https://doi.org/10.5194/bg-2019-488
Preprint. Discussion started: 31 January 2020

DiTullio, G. R., Grebmeier, J. M., Arrigo, K. R., Lizotte, M. P., Robinson, D. H., Leventer, A., Barry, J. P., VanWoert, M. L., and Dunbar, R. B.: Rapid and early export of *Phaeocystis antarctica* blooms in the Ross Sea, Antarctica, Nature, 404, 595–598, https://doi.org/10.1038/35007061, 2000.

Fanton d'Andon, O., Mangin, A., Lavender, S., Antoine, D., Maritorena, S., Morel, A., Barrot, G., Demaria, J., and Pinnock, S.: GlobColour - the European Service for Ocean Colour, in: Proceedings of the 2009 IEEE International Geoscience & Remote Sensing Symposium, IEEE International Geoscience & Remote Sensing Symposium (IGARSS), ISBN: 9781424433957, 2009.

Feng, Y., Hare, C. E., Rose, J. M., Handy, S. M., DiTullio, G. R., Lee, P. A., Smith, W. O., Peloquin, J., Tozzi, S., Sun, J., Zhang, Y., Dunbar, R. B., Long, M. C., Sohst, B., Lohan, M., and Hutchins, D. A.: Interactive effects of iron, irradiance and CO_2 on Ross Sea phytoplankton, Deep Sea Research Part I: Oceanographic Research Papers, 57, 368–383, https://doi.org/10.1016/j.dsr.2009.10.013, 2010.

Freeman, N. M., Lovenduski, N. S., Munro, D. R., Krumhardt, K. M., Lindsay, K., Long, M. C., and Maclennan, M.: The variable and changing Southern Ocean silicate front: Insights from the CESM large ensemble, Global Biogeochemical Cycles, 32, 752–768, https://doi.org/10.1029/2017GB005816, 2018.

Garcia, H. E., Locarnini, R. A., Boyer, T. P., Antonov, J. I., Baranova, O., Zweng, M., Reagan, J., and Johnson, D.: World Ocean Atlas 2013, Volume 3: Dissolved oxygen, apparent oxygen utilization, and oxygen saturation, NOAA Atlas NESDIS 75, 3, 27 pp, 2014a.

Garcia, H. E., Locarnini, R. A., Boyer, T. P., Antonov, J. I., Baranova, O. K., Zweng, M. M., Reagan, J. R., and Johnson, D. R.: World Ocean Atlas 2013, Volume 4 : Dissolved inorganic nutrients (phosphate, nitrate, silicate), NOAA Atlas NESDIS 76, 4, 25 pp, 2014b.

Garcia, N. S., Sedwick, P. N., and DiTullio, G. R.: Influence of irradiance and iron on the growth of colonial *Phaeocystis antarctica*: implications for seasonal bloom dynamics in the Ross Sea, Antarctica, Aquatic Microbial Ecology, 57, 203–220, https://doi.org/10.3354/ame01334, 2009.

Geider, R. J., MacIntyre, H. L., and Kana, T. M.: A dynamic regulatory model of phytoplanktonic acclimation to light, nutrients, and temperature, Limnology and Oceanography, 43, 679–694, https://doi.org/10.4319/lo.1998.43.4.0679, 1998.

Goffart, A., Catalano, G., and Hecq, J.: Factors controlling the distribution of diatoms and *Phaeocystis* in the Ross Sea, Journal of Marine Systems, 27, 161–175, https://doi.org/10.1016/S0924-7963(00)00065-8, 2000.

Gowing, M. M., Garrison, D. L., Kunze, H. B., and Winchell, C. J.: Biological components of Ross Sea short-term particle fluxes in the austral summer of 1995–1996, Deep Sea Research Part I: Oceanographic Research Papers, 48, 2645–2671, https://doi.org/10.1016/S0967-0637(01)00034-6, 2001.

Granéli, E., Granéli, W., Rabbani, M. M., Daugbjerg, N., Fransz, G., Roudy, J. C., and Alder, V. A.: The influence of copepod and krill grazing on the species composition of phytoplankton communities from the Scotia Weddell sea, Polar Biology, 13, 201–213, https://doi.org/10.1007/BF00238930, 1993.

Gravalosa, J. M., Flores, J.-A., Sierro, F. J., and Gersonde, R.: Sea surface distribution of coccolithophores in the eastern Pacific sector of the Southern Ocean (Bellingshausen and Amundsen Seas) during the late austral summer of 2001, Marine Micropaleontology, 69, 16–25, https://doi.org/10.1016/j.marmicro.2007.11.006, 2008.

Green, S. E. and Sambrotto, R. N.: Plankton community structure and export of C, N, P and Si in the Antarctic Circumpolar Current, Deep Sea Research Part II: Topical Studies in Oceanography, 53, 620–643, https://doi.org/10.1016/j.dsr2.2006.01.022, 2006.

Hamm, C. E., Simson, D. A., Merkel, R., and Smetacek, V.: Colonies of *Phaeocystis globosa* are protected by a thin but tough skin, Marine Ecology Progress Series, 187, 101–111, https://doi.org/10.3354/meps187101, 1999.

Hancock, A. M., Davidson, A. T., McKinlay, J., McMinn, A., Schulz, K. G., and van den Enden, R. L.: Ocean acidification changes the structure of an Antarctic coastal protistan community, Biogeosciences, 15, 2393–2410, https://doi.org/10.5194/bg-15-2393-2018, 2018.

https://doi.org/10.5194/bg-2019-488
Preprint. Discussion started: 31 January 2020

Hashioka, T., Vogt, M., Yamanaka, Y., Le Quéré, C., Buitenhuis, E. T., Aita, M. N., Alvain, S., Bopp, L., Hirata, T., Lima, I., Sailley, S., and Doney, S. C.: Phytoplankton competition during the spring bloom in four plankton functional type models, Biogeosciences, 10, 6833–6850, https://doi.org/10.5194/bg-10-6833-2013, 2013.

Haumann, F. A.: Southern Ocean response to recent changes in surface freshwater fluxes, PhD Thesis, ETH Zürich, https://doi.org/10.3929/ethz-b-000166276, 2016.

IPCC: Climate change 2013 - The physical science basis: Working group I contribution to the fifth assessment report of the Intergovernmental Panel on Climate Change, Cambridge University Press, https://doi.org/10.1017/CBO9781107415324, 2014.

Johnson, R., Strutton, P. G., Wright, S. W., McMinn, A., and Meiners, K. M.: Three improved satellite chlorophyll algorithms for the Southern Ocean, Journal of Geophysical Research-Oceans, 118, 3694–3703, https://doi.org/10.1002/jgrc.20270, 2013.

Kaufman, D. E., Friedrichs, M. A. M., Smith, W. O., Hofmann, E. E., Dinniman, M. S., and Hemmings, J. C. P.: Climate change impacts on southern Ross Sea phytoplankton composition, productivity, and export, Journal of Geophysical Research: Oceans, 122, 2339–2359, https://doi.org/10.1002/2016JC012514, 2017.

Keller, M. D., Bellows, W. K., and Guillard, R. R. L.: Dimethyl sulfide production in marine phytoplankton, in: Biogenic Sulfur in the Environment, edited by Saltzman, E. S. and Cooper, W. J., vol. 393 of *ACS Symposium Series*, pp. 167–182, American Chemical Society, https://doi.org/10.1021/bk-1989-0393, ISBN: 0-8412-1612-6, 1989.

Lam, P. J. and Bishop, J. K. B.: High biomass, low export regimes in the Southern Ocean, Deep Sea Research Part II: Topical Studies in Oceanography, 54, 601–638, https://doi.org/10.1016/j.dsr2.2007.01.013, 2007.

Lana, A., Bell, T. G., Simó, R., Vallina, S. M., Ballabrera-Poy, J., Kettle, A. J., Dachs, J., Bopp, L., Saltzman, E. S., Stefels, J., Johnson, J. E., and Liss, P. S.: An updated climatology of surface dimethlysulfide concentrations and emission fluxes in the global ocean, Global Biogeochemical Cycles, 25, 1–17, https://doi.org/10.1029/2010GB003850, 2011.

Laufkötter, C., Vogt, M., Gruber, N., Aumont, O., Bopp, L., Doney, S. C., Dunne, J. P., Hauck, J., John, J. G., Lima, I. D., Seferian, R., and Völker, C.: Projected decreases in future marine export production: the role of the carbon flux through the upper ocean ecosystem, Biogeosciences, 13, 4023–4047, https://doi.org/10.5194/bg-13-4023-2016, 2016.

Lauvset, S. K., Key, R. M., Olsen, A., Van Heuven, S., Velo, A., Lin, X., Schirnick, C., Kozyr, A., Tanhua, T., Hoppema, M., Jutterström, S., Steinfeldt, R., Jeansson, E., Ishii, M., Perez, F. F., Suzuki, T., and Watelet, S.: A new global interior ocean mapped climatology: The 1°x1° GLODAP version 2, Earth System Science Data, 8, 325–340, https://doi.org/10.5194/essd-8-325-2016, 2016.

Le Quéré, C., Buitenhuis, E. T., Moriarty, R., Alvain, S., Aumont, O., Bopp, L., Chollet, S., Enright, C., Franklin, D. J., Geider, R. J., Harrison, S. P., Hirst, A. G., Larsen, S., Legendre, L., Platt, T., Prentice, I. C., Rivkin, R. B., Sailley, S., Sathyendranath, S., Stephens, N., Vogt, M., and Vallina, S. M.: Role of zooplankton dynamics for Southern Ocean phytoplankton biomass and global biogeochemical cycles, Biogeosciences, 13, 4111–4133, https://doi.org/10.5194/bg-13-4111-2016, 2016.

Leblanc, K., Arístegui, J., Armand, L., Assmy, P., Beker, B., Bode, A., Breton, E., Cornet, V., Gibson, J., Gosselin, M.-P., Kopczynska, E., Marshall, H., Peloquin, J., Piontkovski, S., Poulton, A. J., Quéguiner, B., Schiebel, R., Shipe, R., Stefels, J., van Leeuwe, M. A., Varela, M., Widdicombe, C., and Yallop, M.: A global diatom database - abundance, biovolume and biomass in the world ocean, Earth System Science Data, 4, 149–165, https://doi.org/10.5194/essd-4-149-2012, 2012.

Lima, I. D., Lam, P. J., and Doney, S. C.: Dynamics of particulate organic carbon flux in a global ocean model, Biogeosciences, 11, 1177–1198, https://doi.org/10.5194/bg-11-1177-2014, 2014.

Liss, P. S., Malin, G., Turner, S. M., and Holligan, P. M.: Dimethyl sulphide and *Phaeocystis*: A review, Journal of Marine Systems, 5, 41–53, https://doi.org/10.1016/0924-7963(94)90015-9, 1994.

https://doi.org/10.5194/bg-2019-488
Preprint. Discussion started: 31 January 2020

Locarnini, R. A., Mishonov, A. V., Antonov, J. I., Boyer, T. P., Garcia, H. E., Baranova, O. K., Zweng, M. M., Paver, C. R., Reagan, J. R., Johnson, D. R., Hamilton, M., and Seidov, D.: World Ocean Atlas 2013, Volume 1: Temperature, NOAA Atlas NESDIS 73, 1, 40 pp, 2013.

Margalef, R.: Life-forms of phytoplankton as survival alternatives in an unstable environment, Oceanologica Acta, 1, 493–509, 1978.

Maritorena, S., Fanton D'Andon, O., Mangin, A., and Siegel, D. A.: Merged satellite ocean color data products using a bio-optical model: Characteristics, benefits and issues, Remote Sensing of Environment, 114, 1791–1804, https://doi.org/10.1016/j.rse.2010.04.002, 2010.

Martin, J. H., Fitzwater, S. E., and Gordon, R. M.: Iron deficiency limits phytoplankton growth in Antarctic waters, Global Biogeochemical Cycles, 4, 5–12, https://doi.org/10.1029/GB004i001p00005, 1990a.

Martin, J. H., Gordon, R. M., and Fitzwater, S. E.: Iron in Antarctic waters, Nature, 345, 156–158, https://doi.org/10.1038/345156a0, 1990b.

Martínez-García, A., Sigman, D. M., Ren, H., Anderson, R. F., Straub, M., Hodell, D. a., Jaccard, S. L., Eglinton, T. I., and Haug, G. H.: Iron fertilization of the Subantarctic ocean during the last ice age., Science, 343, 1347–50, https://doi.org/10.1126/science.1246848, 2014.

Mills, M. M., Kropuenske, L. R., van Dijken, G. L., Alderkamp, A.-C., Berg, G. M., Robinson, D. H., Welschmeyer, N. A., and Arrigo, K. R.: Photophysiology in two Southern Ocean phytoplankton taxa: photosynthesis of *Phaeocystis Antarctica* (Prymnesiophyceae) and *Fragilariopsis cylindrus* (Bacillariophyceae) under simulated mixed-layer irradiance, Journal of Phycology, 46, 1114–1127, https://doi.org/10.1111/j.1529-8817.2010.00923.x, 2010.

Moore, J. K., Lindsay, K., Doney, S. C., Long, M. C., and Misumi, K.: Marine ecosystem dynamics and biogeochemical cycling in the Community Earth System Model [CESM1(BGC)]: Comparison of the 1990s with the 2090s under the RCP4.5 and RCP8.5 scenarios, Journal of Climate, 26, 9291–9312, https://doi.org/10.1175/JCLI-D-12-00566.1, 2013.

Morel, A. and Berthon, J.-F.: Surface pigments, algal biomass profiles, and potential production of the euphotic layer: Relationships reinvestigated in view of remote-sensing applications, Limnology and Oceanography, 34, 1545–1562, https://doi.org/10.4319/lo.1989.34.8.1545, 1989.

NASA-OBPG: NASA Goddard Space Flight Center, Ocean Ecology Laboratory, Ocean Biology Processing Group, Moderate-resolution Imaging Spectroradiometer (MODIS) Aqua Chlorophyll Data, https://doi.org/10.5067/AQUA/MODIS/L3M/CHL/2014, 2014a.

NASA-OBPG: NASA Goddard Space Flight Center, Ocean Ecology Laboratory, Ocean Biology Processing Group, Sea-viewing Wide Field-of-view Sensor (SeaWiFS) Chlorophyll Data, https://doi.org/10.5067/ORBVIEW-2/SEAWIFS/L3M/CHL/2014, 2014b.

Nejstgaard, J. C., Tang, K. W., Steinke, M., Dutz, J., Koski, M., Antajan, E., and Long, J. D.: Zooplankton grazing on *Phaeocystis*: a quantitative review and future challenges, in: *Phaeocystis*, major link in the biogeochemical cycling of climate-relevant elements, vol. 83, pp. 147–172, Springer Netherlands, https://doi.org/10.1007/s10533-007-9098-y, 2007.

Nguyen, B. C., Mihalopoulos, N., and Belviso, S.: Seasonal variation of atmospheric dimethylsulfide at Amsterdam Island in the southern Indian Ocean, Journal of Atmospheric Chemistry, 11, 123–141, https://doi.org/10.1007/BF00053671, 1990.

Nissen, C., Vogt, M., Münnich, M., Gruber, N., and Haumann, F. A.: Factors controlling coccolithophore biogeography in the Southern Ocean, Biogeosciences, 15, 6997–7024, https://doi.org/10.5194/bg-15-6997-2018, 2018.

O'Brien, C. J., Peloquin, J. A., Vogt, M., Heinle, M., Gruber, N., Ajani, P., Andruleit, H., Arístegui, J., Beaufort, L., Estrada, M., Karentz, D., Kopczyńska, E., Lee, R., Poulton, A. J., Pritchard, T., and Widdicombe, C.: Global marine plankton functional type biomass distributions: coccolithophores, Earth System Science Data, 5, 259–276, https://doi.org/10.5194/essd-5-259-2013, 2013.

O'Malley, R.: Ocean Productivity website, data downloaded from http://www.science.oregonstate.edu/ocean.productivity/index.php, last access: 16 May 2016.

https://doi.org/10.5194/bg-2019-488
Preprint. Discussion started: 31 January 2020

Palter, J. B., Sarmiento, J. L., Gnanadesikan, A., Simeon, J., and Slater, R. D.: Fueling export production: nutrient return pathways from the deep ocean and their dependence on the Meridional Overturning Circulation, Biogeosciences, 7, 3549–3568, https://doi.org/10.5194/bg-7-3549-2010, 2010.

Pasquer, B., Laruelle, G., Becquevort, S., Schoemann, V., Goosse, H., and Lancelot, C.: Linking ocean biogeochemical cycles and ecosystem structure and function: results of the complex SWAMCO-4 model, Journal of Sea Research, 53, 93–108, https://doi.org/10.1016/j.seares.2004.07.001, 2005.

Peloquin, J. A. and Smith, W. O.: Phytoplankton blooms in the Ross Sea, Antarctica: Interannual variability in magnitude, temporal patterns, and composition, Journal of Geophysical Research, 112, C08 013, https://doi.org/10.1029/2006JC003816, 2007.

Peperzak, L.: Observations of flagellates in colonies of *Phaeocystis globosa* (Prymnesiophyceae); a hypothesis for their position in the life cycle, Journal of Plankton Research, 22, 2181–2203, https://doi.org/10.1093/plankt/22.12.2181, 2000.

Popova, E. E., Pollard, R. T., Lucas, M. I., Venables, H. J., and Anderson, T. R.: Real-time forecasting of ecosystem dynamics during the CROZEX experiment and the roles of light, iron, silicate, and circulation, Deep Sea Research Part II: Topical Studies in Oceanography, 54, 1966–1988, https://doi.org/10.1016/j.dsr2.2007.06.018, 2007.

Poulton, A. J., Moore, M. C., Seeyave, S., Lucas, M. I., Fielding, S., and Ward, P.: Phytoplankton community composition around the Crozet Plateau, with emphasis on diatoms and *Phaeocystis*, Deep Sea Research Part II: Topical Studies in Oceanography, 54, 2085–2105, https://doi.org/10.1016/j.dsr2.2007.06.005, 2007.

Reigstad, M. and Wassmann, P.: Does *Phaeocystis* spp. contribute significantly to vertical export of organic carbon?, in: *Phaeocystis*, major link in the biogeochemical cycling of climate-relevant elements, vol. 83, pp. 217–234, Springer Netherlands, https://doi.org/10.1007/978-1-4020-6214-8_16, http://link.springer.com/10.1007/978-1-4020-6214-8_16, 2007.

Reynolds, C. S.: The Ecology of Phytoplankton, Cambridge University Press, Cambridge, https://doi.org/10.1017/CBO9780511542145, https://www.cambridge.org/core/product/identifier/9780511542145/type/book, ISBN: 9780511542145, 2006.

Rivero-Calle, S., Gnanadesikan, A., Del Castillo, C. E., Balch, W. M., and Guikema, S. D.: Multidecadal increase in North Atlantic coccolithophores and the potential role of rising CO_2, Science, 350, 1533–1537, https://doi.org/10.1126/science.aaa8026, 2015.

Rousseau, V., Vaulot, D., Casotti, R., Cariou, V., Lenz, J., Gunkel, J., and Baumann, M.: The life cycle of *Phaeocystis* (Prymnesiophycaea): evidence and hypotheses, Journal of Marine Systems, 5, 23–39, https://doi.org/10.1016/0924-7963(94)90014-0, 1994.

Saavedra-Pellitero, M., Baumann, K.-H., Flores, J.-A., and Gersonde, R.: Biogeographic distribution of living coccolithophores in the Pacific sector of the Southern Ocean, Marine Micropaleontology, 109, 1–20, https://doi.org/10.1016/j.marmicro.2014.03.003, 2014.

Sarmiento, J. L., Gruber, N., Brzezinski, M. A., and Dunne, J. P.: High-latitude controls of thermocline nutrients and low latitude biological productivity., Nature, 427, 56–60, https://doi.org/10.1038/nature02127, 2004.

Sathyendranath, S., Stuart, V., Nair, A., Oka, K., Nakane, T., Bouman, H., Forget, M. H., Maass, H., and Platt, T.: Carbon-to-chlorophyll ratio and growth rate of phytoplankton in the sea, Marine Ecology Progress Series, 383, 73–84, https://doi.org/10.3354/meps07998, 2009.

Schlitzer, R.: Export production in the Equatorial and North Pacific derived from dissolved oxygen, nutrient and carbon data, J. Oceanogr., 60, 53–62, https://doi.org/10.1023/B:JOCE.0000038318.38916.e6, 2004.

Schoemann, V., Wollast, R., Chou, L., and Lancelot, C.: Effects of photosynthesis on the accumulation of Mn and Fe by *Phaeocystis* colonies, Limnology and Oceanography, 46, 1065–1076, https://doi.org/10.4319/lo.2001.46.5.1065, 2001.

Schoemann, V., Becquevort, S., Stefels, J., Rousseau, V., and Lancelot, C.: *Phaeocystis* blooms in the global ocean and their controlling mechanisms: a review, Journal of Sea Research, 53, 43–66, https://doi.org/10.1016/j.seares.2004.01.008, 2005.

https://doi.org/10.5194/bg-2019-488
Preprint. Discussion started: 31 January 2020

Sedwick, P. N., DiTullio, G. R., and Mackey, D. J.: Iron and manganese in the Ross Sea, Antarctica: Seasonal iron limitation in Antarctic shelf waters, Journal of Geophysical Research, 105, 11 321, https://doi.org/10.1029/2000JC000256, 2000.

Sedwick, P. N., Garcia, N. S., Riseman, S. F., Marsay, C. M., and DiTullio, G. R.: Evidence for high iron requirements of colonial *Phaeocystis antarctica* at low irradiance, in: *Phaeocystis*, major link in the biogeochemical cycling of climate-relevant elements, vol. 83, pp. 83–97, Springer Netherlands, https://doi.org/10.1007/978-1-4020-6214-8_8, 2007.

Shchepetkin, A. F. and McWilliams, J. C.: The regional oceanic modeling system (ROMS): a split-explicit, free-surface, topography-following-coordinate oceanic model, Ocean Modeling, 9, 347–404, https://doi.org/10.1016/j.ocemod.2004.08.002, 2005.

Simó, R. and Pedrós-Alló, C.: Role of vertical mixing in controlling the oceanic production of dimethyl sulphide, Nature, 402, 396–399, https://doi.org/10.1038/46516, 1999.

Smetacek, V., Assmy, P., and Henjes, J.: The role of grazing in structuring Southern Ocean pelagic ecosystems and biogeochemical cycles, Antarct. Sci., 16, 541–558, https://doi.org/10.1017/S0954102004002317, 2004.

Smith, W. O. and Gordon, L. I.: Hyperproductivity of the Ross Sea (Antarctica) polynya during austral spring, Geophysical Research Letters, 24, 233–236, https://doi.org/10.1029/96GL03926, 1997.

Smith, W. O., Dennett, M. R., Mathot, S., and Caron, D. A.: The temporal dynamics of the flagellated and colonial stages of *Phaeocystis antarctica* in the Ross Sea, Deep Sea Research Part II: Topical Studies in Oceanography, 50, 605–617, https://doi.org/10.1016/S0967-0645(02)00586-6, 2003.

Smith, W. O., Dinniman, M. S., Tozzi, S., DiTullio, G. R., Mangoni, O., Modigh, M., and Saggiomo, V.: Phytoplankton photosynthetic pigments in the Ross Sea: Patterns and relationships among functional groups, Journal of Marine Systems, 82, 177–185, https://doi.org/10.1016/j.jmarsys.2010.04.014, 2010.

Smith, W. O., Shields, A. R., Dreyer, J. C., Peloquin, J. A., and A., V.: Interannual variability in vertical export in the Ross Sea: Magnitude, composition, and environmental correlates, Deep Sea Research Part I: Oceanographic Research Papers, 58, 147–159, https://doi.org/10.1016/j.dsr.2010.11.007, 2011.

Smith, W. O., Ainley, D. G., Arrigo, K. R., and Dinniman, M. S.: The Oceanography and Ecology of the Ross Sea, Annual Review of Marine Science, 6, 469–487, https://doi.org/10.1146/annurev-marine-010213-135114, 2014.

Soppa, M., Hirata, T., Silva, B., Dinter, T., Peeken, I., Wiegmann, S., and Bracher, A.: Global retrieval of diatom abundance based on phytoplankton pigments and satellite data, Remote Sensing, 6, 10 089–10 106, https://doi.org/10.3390/rs61010089, 2014.

Soppa, M., Völker, C., and Bracher, A.: Diatom phenology in the Southern Ocean: mean patterns, trends and the role of climate Oscillations, Remote Sensing, 8, 420, https://doi.org/10.3390/rs8050420, 2016.

Stange, P., Bach, L. T., Le Moigne, F. A. C., Taucher, J., Boxhammer, T., and Riebesell, U.: Quantifying the time lag between organic matter production and export in the surface ocean: Implications for estimates of export efficiency, Geophysical Research Letters, 44, 268–276, https://doi.org/10.1002/2016GL070875, 2017.

Stefels, J., Steinke, M., Turner, S., Malin, G., and Belviso, S.: Environmental constraints on the production and removal of the climatically active gas dimethylsulphide (DMS) and implications for ecosystem modelling, in: *Phaeocystis*, major link in the biogeochemical cycling of climate-relevant elements, pp. 245–275, Springer Netherlands, https://doi.org/10.1007/978-1-4020-6214-8_18, 2007.

Steinberg, D. K. and Landry, M. R.: Zooplankton and the ocean carbon cycle, Annual Review of Marine Science, 9, 413–444, https://doi.org/10.1146/annurev-marine-010814-015924, 2017.

Swan, C. M., Vogt, M., Gruber, N., and Laufkötter, C.: A global seasonal surface ocean climatology of phytoplankton types based on CHEMTAX analysis of HPLC pigments, Deep-Sea Research Part I, 109, 137–156, https://doi.org/10.1016/j.dsr.2015.12.002, 2016.

https://doi.org/10.5194/bg-2019-488
Preprint. Discussion started: 31 January 2020

Tagliabue, A. and Arrigo, K. R.: Iron in the Ross Sea: 1. Impact on CO_2 fluxes via variation in phytoplankton functional group and non-Redfield stoichiometry, Journal of Geophysical Research: Oceans, 110, 1–15, https://doi.org/10.1029/2004JC002531, 2005.

Tang, K. W., Smith, W. O., Elliott, D. T., and Shields, A. R.: Colony size of *Phaeocystis Antarctica* (Prymnesiophyceae) as influenced by zooplankton grazers, Journal of Phycology, 44, 1372–1378, https://doi.org/10.1111/j.1529-8817.2008.00595.x, 2008.

Tang, K. W., Smith, W. O., Shields, A. R., and Elliott, D. T.: Survival and recovery of *Phaeocystis antarctica* (Prymnesiophyceae) from prolonged darkness and freezing, Proceedings of the Royal Society B: Biological Sciences, 276, 81–90, https://doi.org/10.1098/rspb.2008.0598, 2009.

Thomalla, S. J., Racault, M.-F., Swart, S., and Monteiro, P. M. S.: High-resolution view of the spring bloom initiation and net community production in the Subantarctic Southern Ocean using glider data, ICES Journal of Marine Science: Journal du Conseil, 72, 1999–2020, https://doi.org/10.1093/icesjms/fsv105, 2015.

Timmermans, K. R., van der Wagt, B., and de Baar, H. J. W.: Growth rates, half saturation constants, and silicate, nitrate, and phosphate depletion in relation to iron availability of four large open-ocean diatoms from the Southern Ocean, Limnology and Oceanography, 49, 2141–2151, https://doi.org/10.4319/lo.2004.49.6.2141, 2004.

Tyrrell, T. and Charalampopoulou, A.: Coccolithophore size, abundance and calcification across Drake Passage (Southern Ocean), 2009, https://doi.org/10.1594/PANGAEA.771715, 2009.

van Boekel, W. H. M., Hansen, F. C., Riegman, R., and Bak, R. P. M.: Lysis-induced decline of a *Phaeocystis* spring bloom and coupling with the microbial foodweb, Marine Ecology Progress Series, 81, 269–276, https://doi.org/10.3354/meps081269, 1992.

van Hilst, C. M. and Smith, W. O.: Photosynthesis/irradiance relationships in the Ross Sea, Antarctica, and their control by phytoplankton assemblage composition and environmental factors, Marine Ecology Progress Series, 226, 1–12, https://doi.org/10.3354/meps226001, 2002.

Veldhuis, M. J. W., Colijn, F., and Admiraal, W.: Phosphate Utilization in *Phaeocystis pouchetii* (*Haptophyceae*), Marine Ecology, 12, 53–62, https://doi.org/10.1111/j.1439-0485.1991.tb00083.x, 1991.

Verity, P. G.: Grazing experiments and model simulations of the role of zooplankton in *Phaeocystis* food webs, Journal of Sea Research, 43, 317–343, https://doi.org/10.1016/S1385-1101(00)00025-3, 2000.

Vogt, M., O'Brien, C., Peloquin, J., Schoemann, V., Breton, E., Estrada, M., Gibson, J., Karentz, D., Van Leeuwe, M. A., Stefels, J., Widdicombe, C., and Peperzak, L.: Global marine plankton functional type biomass distributions: *Phaeocystis* spp., Earth System Science Data, 4, 107–120, https://doi.org/10.5194/essd-4-107-2012, 2012.

Wang, S. and Moore, J. K.: Incorporating *Phaeocystis* into a Southern Ocean ecosystem model, Journal of Geophysical Research, 116, C01 019, https://doi.org/10.1029/2009JC005817, 2011.

Wang, S., Elliott, S., Maltrud, M., and Cameron-Smith, P.: Influence of explicit *Phaeocystis* parameterizations on the global distribution of marine dimethyl sulfide, Journal of Geophysical Research: Biogeosciences, 120, 2158–2177, https://doi.org/10.1002/2015JG003017, 2015.

Winter, A., Henderiks, J., Beaufort, L., Rickaby, R. E. M., and Brown, C. W.: Poleward expansion of the coccolithophore *Emiliania huxleyi*, Journal of Plankton Research, 36, 316–325, https://doi.org/10.1093/plankt/fbt110, 2013.

Wright, S. W., van den Enden, R. L., Pearce, I., Davidson, A. T., Scott, F. J., and Westwood, K. J.: Phytoplankton community structure and stocks in the Southern Ocean (30-80°E) determined by CHEMTAX analysis of HPLC pigment signatures, Deep-Sea Research Part II, 57, 758–778, https://doi.org/10.1016/j.dsr2.2009.06.015, 2010.

https://doi.org/10.5194/bg-2019-488
Preprint. Discussion started: 31 January 2020

Yang, S., Gruber, N., Long, M. C., and Vogt, M.: ENSO-driven variability of denitrification and suboxia in the Eastern Tropical Pacific
1025 Ocean, Global Biogeochemical Cycles, 31, 1470–1487, https://doi.org/10.1002/2016GB005596, 2017.

Zweng, M. M., Reagan, J. R., Antonov, J. I., Mishonov, A. V., Boyer, T. P., Garcia, H. E., Baranova, O. K., Johnson, D. R., Seidov, D., and Bidlle, M. M.: World Ocean Atlas 2013, Volume 2: Salinity, NOAA Atlas NESDIS 74, 2, 39 pp, 2013.